PCCP

Physical Chemistry Chemical Physics

www.rsc.org/pccp

Volume 13 | Number 9 | 7 March 2011 | Pages 3561–4164

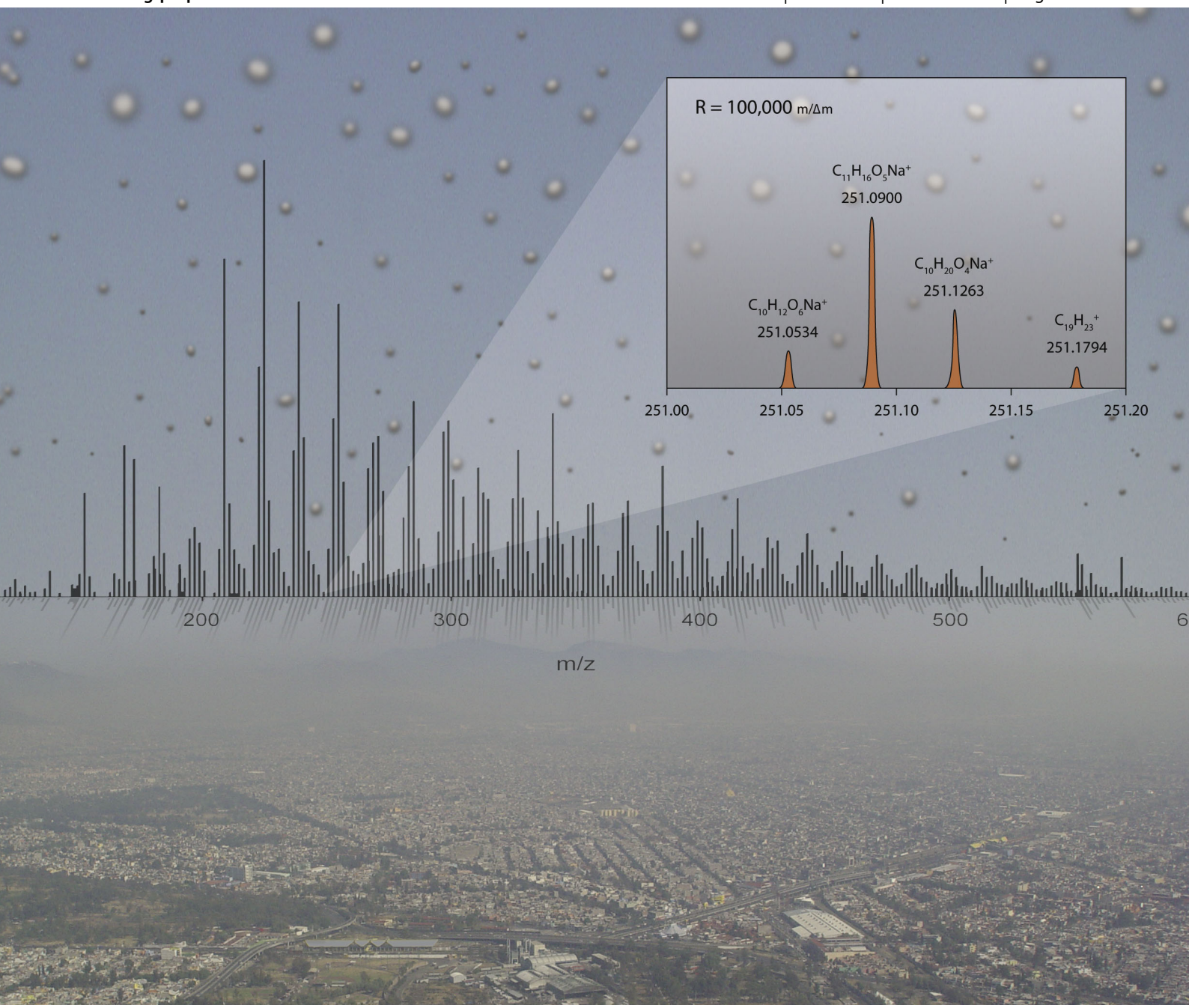

ISSN 1463-9076

COVER ARTICLE
Nizkorodov *et al.*
Molecular chemistry of organic aerosols through the application of high resolution mass spectrometry

HOT ARTICLE
Weingart, Garavelli *et al.*
Product formation in rhodopsin by fast hydrogen motions

PCCP

Dynamic Article Links

Cite this: *Phys. Chem. Chem. Phys.*, 2011, **13**, 3612–3629

www.rsc.org/pccp

PERSPECTIVE

Molecular chemistry of organic aerosols through the application of high resolution mass spectrometry

Sergey A. Nizkorodov,[a] Julia Laskin[b] and Alexander Laskin[c]

Received 4th October 2010, Accepted 11th November 2010
DOI: 10.1039/c0cp02032j

Understanding the molecular composition and fundamental chemical transformations of organic aerosols (OA) during their formation and aging is both a major challenge and the area of great uncertainty in atmospheric research. Particularly, little is known about fundamental relationship between the chemical composition and physicochemical properties of OA, their atmospheric history, evolution, and the impact on the environment. Ambient soft-ionization methods combined with high-resolution mass spectrometry (HR-MS) analysis provide detailed information on the molecular content of OA that is pivotal for improving the understanding of their complex composition, multi-phase aging chemistry, direct (light absorption and scattering) and indirect (aerosol-cloud interactions) effects on atmospheric radiation and climate, health effects. The HR-MS methods can detect thousands of individual OA constituents at once, provide their elemental formulae from accurate mass measurements and structural information based on tandem mass spectrometry. Integration with additional analytical tools, such as chromatography and UV/Vis absorption spectroscopy, makes it possible to further separate OA compounds by their polarity and ability to absorb solar radiation. The goal of this perspective is to describe contemporary HR-MS methods, review recent applications in field and laboratory studies of OA, and explain how the information obtained from HR-MS methods can be translated into an improved understanding of OA chemistry.

[a] *Department of Chemistry, University of California, Irvine, California 92617, USA. E-mail: nizkorod@uci.edu; Fax: (949) 824-1262*
[b] *Chemical and Materials Sciences Division, Pacific Northwest National Laboratory, Richland, Washington 99352, USA. E-mail: julia.laskin@pnl.gov; Fax: (509) 371-6139*
[c] *Environmental Molecular Sciences Laboratory, Pacific Northwest National Laboratory, Richland, Washington 99352, USA. E-mail: alexander.laskin@pnl.gov; Fax: (509) 371-6139*

1. Introduction

The gases N_2, O_2, H_2O, and Ar account for more than 99.9% of the atmospheric content. However, atmospheric chemical processes are primarily driven by molecules present in trace amounts: inorganic compounds such as NO_2, O_3, SO_2, OH,

Sergey A. Nizkorodov, Julia Laskin and Alexander Laskin

Sergey Nizkorodov received his undergraduate education in biochemistry from Novosibirsk State University, Russia (1993) and his graduate education in physical chemistry from Basel University, Switzerland (1997). He became interested in atmospheric chemistry problems during his postdoctoral research appointments, first at the University of Colorado at Boulder, and then at the California Institute of Technology. In 2002, he joined the Chemistry Department at the University of California, Irvine. His current research is on the chemistry and photochemistry of organic aerosols.
Julia Laskin received her MSc degree in Physics from the Leningrad Polytechnical Institute in 1990 and her PhD degree in physical chemistry from the Hebrew University of Jerusalem in 1998. After a postdoc at the University of Delaware and Pacific Northwest National Laboratory (PNNL) she became a permanent PNNL staff member in 2003. Her research is focused on the fundamental understanding of phenomena underlying the analysis of complex molecules using high-resolution mass spectrometry.
Alexander Laskin received his MS degree (physics) in 1991 from the Leningrad Polytechnical Institute, Russia, and PhD degree (physical chemistry) in 1998 from the Hebrew University of Jerusalem, Israel. His graduate research and postdoctoral research in University of Delaware included studies on chemical kinetics and combustion chemistry. In 1999, he joined the PNNL staff to conduct research into atmospheric aerosol chemistry. His present and past research interests include: physical and analytical chemistry of environmental aerosols, novel methods of aerosol collection and analysis, microscopy and microanalysis of aerosols, the environmental impact of aerosols, combustion chemistry, combustion related aerosols and chemical kinetics.

This journal is © the Owner Societies 2011

HO_2, *etc.* and organic compounds such as non-methane hydrocarbons, terpenoids, aromatic compounds, dimethyl sulfide, *etc.* Most trace species are present in the air in a gaseous form but a fraction of them have sufficiently low volatilities to accumulate into particles giving rise to aerosols, which can also be classified as inorganic and organic depending on the prevailing type of the aerosol molecular constituents. The amount of material residing in particles is small, of the order of 1 μg m^{-3} or 10^{-7}% by mass (for reference, 1 m^3 of standard air weighs about 1.2 kg). Nevertheless, aerosols have profound effect on the energy balance in the atmosphere because they can absorb and scatter solar radiation and reversibly take up water forming cloud droplets, thus controlling the planet's albedo.[1] Elevated concentrations of aerosols in urban areas contribute to visibility degradation and pose significant health risks.[2] Environmental effects of aerosols have been driving research on chemical and physical processes resulting in formation of airborne particulates since the early 50's.[3,4]

Molecular composition of organic aerosols (OA) is remarkably complex. Primary organic aerosols (POA) are emitted directly by anthropogenic and natural sources such as fossil fuel combustion and biomass burning, which are known to generate particulates with a high degree of chemical heterogeneity. Secondary organic aerosols (SOA) are "assembled" in air from condensable products of atmospheric oxidation of various volatile organic compounds (VOCs).[5] Even a single VOC can give rise to thousands of different products because of the highly-branched free radical mechanisms of oxidation. The aerosol composition continues to change long after the initial particle formation as a result of chemical reactions between particle constituents, reactive uptake of gas-phase molecules by the particle, direct photochemical processes inside the particle, and condensation and evaporation of water on the particle.[6–9] These processes contribute to chemical "aging" that takes place on a time scale ranging from minutes to days, and may significantly change molecular composition of particles before their removal from the atmosphere. Organic particles sampled from ambient air thus contain thousands of chemically distinct organic compounds.

Identification and quantification of molecular markers of different types of OA or specific classes of molecules in OA have always played an important role in understanding the sources and the mechanisms of particle formation and subsequent chemical aging. For example, hopanes are routinely used as unique molecular markers of vehicular exhaust, and levoglucosan is a marker for biomass burning aerosols (BBA). Occurrence of several tetrols in OA from the Amazonian rain forest has served as a proof that isoprene is a significant aerosol precursor.[10] Observation of organosulfates in chamber studies and in the field demonstrated the importance of sulfuric acid esterification reactions in aerosols.[11,12] There are numerous other examples of new chemistry discovered by the detection and molecular characterization of individual compounds in OA.

The analysis of the molecular markers of OA typically requires a combination of sophisticated extraction and separation methods with highly specific detectors. By appropriately optimizing the separation and detection approaches, the molecules of interest can be observed without significant interference from other OA constituents. The alternative approach, which has been gaining popularity in recent years, is to forgo separation entirely and attempt to identify as many species in OA as possible. This has been the philosophy behind the development of various types of aerosol mass spectrometry instruments.[13–20] A typical aerosol mass spectrometer vaporizes the entire particle with a laser blast or with heat, and ionizes the resulting vapor with electron impact, pulsed radiation, or ion-molecule chemistry. A number of classes of molecules can be identified simultaneously, sometimes on a particle-by-particle basis.

Most of the currently available aerosol mass spectrometers rely on "hard" ionization methods, and therefore observe ionic fragments.[17] A "soft" ionization method that converts the precursor molecules into positive or negative ions without fragmentation is a key prerequisite for the molecular assignment of organic compounds, which fragment rather extensively under the traditional electron impact ionization conditions. As discussed in more detail below, a number of soft ionization methods have been developed in recent years, and successfully coupled with high resolution mass spectrometers.

Chemical characterization of aerosol constituents using mass spectrometry shares many common challenges with the analysis of petroleum[21] and dissolved organic matter (DOM),[22] which also contain a complex mixture of organic compounds with a wide range of molecular weights, structures, physical properties and chemical reactivity. The complexity of these environmental samples has prompted the development of high-resolution mass analysis approaches capable of resolving small mass differences (<0.001 m/z) over a broad m/z range. When combined with soft ionization techniques, high-resolution mass spectrometry (HR-MS) becomes a powerful tool for detailed characterization of such complex samples.[23] For example, one of the recent studies resolved and identified over 30 000 individual components of petroleum using HR-MS.[24] Elemental formulae of petroleum components are usually assigned as $C_cH_hN_nO_oS_s$ (c unlimited, h unlimited, $0 < n < 5$, $0 < o < 10$, and $0 < s < 2$).[25] Similar to petroleum samples, most aerosol constituents are observed in mass spectra as singly charged ions with $m/z < 1000$. However, elemental assignment of OA constituents requires incorporation of a considerably larger number of oxygen atoms ($0 < o < 30$) and one sodium cation, which increases the degree of ambiguity in molecular assignments. In addition, recent study[26] demonstrated the presence of complexes of organic molecules with rare earth and transition metals in OA, which further complicates the identification of aerosol constituents.

The application of HR-MS combined with tandem mass spectrometry (MS^n) for structural characterization of OA constituents, pioneered by the group of Murray Johnston (University of Delaware) in 2004,[27] is currently a rapidly growing area of research in aerosol chemistry. Table 1 lists all studies published to date on the HR-MS analysis of OA and relevant rain/fog water samples. For the purposes of this perspective article, we limit our discussion to studies relying on mass resolving power in excess of 50 000.[26–53] The vast

Table 1 Summary of HR-MS studies on the chemical characterization of OA and relevant rain/fog samples

Reference	Analyte	Sample Preparation	Ionization Method, Mass Detector	Resolving Power ($m/\Delta m$)	Comments
Tolocka et al., 2004[27]	α-pinene/O_3 SOA	Solvent extraction: CH_3OH, CH_3CN	Direct infusion ESI (+) FT-ICR (9.4 T)	100 000	Detection of oligomeric products; MS^n analysis of molecular structures of oligomers
Reemtsma et al., 2006[28]	WSOC constituents in ambient aerosol samples	Solvent extraction: acidified H_2O; solid-phase extraction	Direct infusion ESI (±) FT-ICR (6 T)	100 000	Identification of fulvic acids and series of sulfated, nitrated, and mixed sulfated and nitrated molecules in atmospheric aerosol
Reinhardt et al., 2007[29]	α-pinene/O_3 SOA	Solvent extraction: CH_3CN–H_2O	Direct infusion ESI (+) FT-ICR (7 T)	400 000	Analysis of elemental composition of monomers and oligomers; evidence for acetal formation and esterification reactions relevant to SOA formation
Walser et al., 2008[30]	d-limonene/O_3 SOA	Solvent extraction: CH_3CN, CH_3OH, H_2O, Cl_2CH_2	Direct infusion ESI (±) Orbitrap	60 000	Analysis of elemental composition of monomers and oligomers; reaction mechanism of SOA formation
Bateman et al., 2008 [31]	d-limonene/O_3 SOA	Solvent extraction: CH_3CN, CD_3CN, CH_3OH, CD_3OH	Direct infusion ESI (±) Orbitrap	60 000	Solvent–analyte reactivity as a tool for improved characterization of functional groups in SOA constituents
Sadezky et al.,[32]	Enol ether/O_3 alkenes/ O_3 SOA	Solvent extraction: CH_3OH–H_2O	Direct infusion ESI (+) FT-ICR (7 T)	100 000	Molecular characterization of oligomeric products as the main constituents of the SOA; a common formation mechanism is reported; MS^n analysis of molecular structures
Wozniak et al. 2008,[33]	WSOC constituents in ambient aerosol samples	Solvent extraction: acidified H_2O	Direct infusion ESI (+) FT-ICR (12 T)	100 000	Identification of individual molecules with $C_cH_hO_oN_nS_s$ elemental formulae; detection of lignin-like and lipid-like compounds
Gomez-Gonzalez et al., 2008[34]	Samples of ambient aerosol from K-puszta site (Hungary)	Solvent extraction: CH_3OH–H_2O	Direct infusion ESI (−) Orbitrap	100 000	Detection of organosulfates in ambient aerosols; MS^n analysis of selected molecular structures
Altieri et al., 2008[35]	Products of aqueous photooxidation of methylglyoxal	Aqueous extracts	Direct infusion ESI (−) FT-ICR (9.4 T)	> 100 000	Analysis of oligomer products formed through aqueous reactions of methylglyoxal and OH; chemical composition of reaction products; reaction mechanisms
Perri et al., 2009[36]	Products of aqueous photooxidation of glycolaldehyde	Aqueous extracts	Direct infusion ESI (−) FT-ICR (9.4 T)	> 100 000	Analysis of oligomer products formed through aqueous reactions of glycolaldehyde and OH; chemical composition of reaction products, reaction mechanisms.
Muller et al., 2009[37]	α-pinene/O_3 sabinene/ O_3 cyclohexene/O_3 SOA	Solvent extraction: CH_3OH–H_2O	LC-ESI (±) FT-ICR (7 T)	100 000	Analysis of elemental composition of monomers and oligomers; MS^n analysis of molecular structures
Altieri et al., 2009[38]	Rain water samples	Aqueous solution diluted with CH_3OH	Direct infusion ESI (−) FT-ICR (9.4 T)	> 100 000	Analysis of elemental composition of individual species: detection of oligomers, organosulfates, and nitrooxy organosulfates
Bateman et al., 2009[39]	d-limonene/O_3 SOA	Solvent extraction: CH_3CN	Direct infusion ESI (±) Orbitrap	60 000–100 000	Analysis of elemental composition of SOA as a function of particle size, reaction time, UV radiation level and relative humidity
Heaton et al., 2009[40]	α-pinene/O_3 β-pinene/ O_3 SOA	Solvent extraction: CH_3CN–H_2O CH_3OH–H_2O H_2O	Direct infusion ESI (±) FT-ICR (12 T) FT-ICR (7 T)	> 100 000	Analysis of elemental composition of individual species; detection of structural domains that correspond to separate oligomer formation mechanisms
Smith et al., 2009[41]	Biomass burning aerosols (BBA)	Solvent extraction: CH_3OH	Direct infusion ESI (+) Orbitrap	60 000	Assignment of the elemental composition for hundreds of individual compounds; characteristic species as unique markers for different types of biofuels; observation of a significant number of highly oxidized polar species
Laskin, A. et al., 2009[42]	Biomass burning aerosols (BBA)	Solvent extraction: CH_3OH	Direct infusion ESI (+) Orbitrap	60 000	Detailed characterization of N-containing species in BBA based on accurate mass measurements and MS^n fragmentation experiments; detection of a number of N-heterocyclic compounds
Altieri et al., 2009[43]	Ambient rain water samples	Aqueous solution diluted with CH_3OH	Direct infusion ESI (±) FT-ICR (9.4 T)	> 100 000	Elemental compositions of N-containing compounds in rain water; results indicate reduced (basic) functionality of N-containing compounds
Nguyen et al., 2010[44]	Isoprene/O_3 SOA	Solvent extraction: CH_3CN	Direct infusion ESI (±) Orbitrap	60 000	Analysis of elemental composition of individual constituents of SOA; formaldehyde (CH_2O) identified as a building block in oligomerization; visualization of HR-MS data using VK *vs.* DBE diagrams
Laskin, J. et al., 2010[45]	d-limonene/O_3 SOA; fresh *versus* aged with NH_3 (g) samples	Substrate deposited samples of SOA	DESI (+) Orbitrap	60 000	Application of DESI/HR-MS for detailed chemical characterization and studies of chemical aging of SOA; detection of N-containing species in SOA aged with NH_3; MS^n analysis of molecular structures

This journal is © the Owner Societies 2011

Table 1 (*continued*)

Reference	Analyte	Sample Preparation	Ionization Method, Mass Detector	Resolving Power ($m/\Delta m$)	Comments
Mazzoleni et al., 2010[46]	Ambient fog water samples	Aqueous solution; solid phase extraction	Direct infusion ESI (−) FT-ICR (9.4 T)	200 000	Analysis of elemental composition of organic nitrogen, sulfur, and nitrogen-sulfur compounds
Perri et al., 2009[47]	Products of aqueous photolysis of glycolaldehyde/H_2SO_4 H_2O_2 mixture	Aqueous extracts	Direct infusion ESI (−) FT-ICR (9.4 T)	> 100 000	Analysis of oligomer products formed through aqueous reactions of glycolaldehyde and OH in the presence of sulfate ions; chemical composition of reaction products; detection of organosulfates; reaction mechanism
Roach et al., 2010[48]	d-limonene/O_3 SOA; fresh *versus* aged with NH_3 (g) samples Biomass burning aerosols (BBA) Samples of ambient aerosols from Mexico City	Substrate deposited samples of aerosols	Nano-DESI (+) Orbitrap	60 000	Application of nano-DESI/HR-MS for molecular-level chemical characterization of OA; fast and efficient characterization of OA collected on substrates without sample preparation using < 10 ng of material; detection of N-containing oligomeric products in Mexico City PM samples
Hall and Johnston, 2010[49]	α-pinene/O_3 SOA	Solvent extraction: CH_3CN CH_3OH H_2O	Direct infusion ESI (±) FT-ICR (7 T)	100 000	Extraction efficiency, and molecular composition of individual oligomeric species in SOA; quantitative estimates of monomers (<50%) and oligomers (>50%) contributions to the total SOA mass
Bateman et al., 2010[50]	WSOC of d-limonene/O_3 SOA WSOC of biomass burning aerosols (BBA)	Solvent extraction: CH_3CN H_2O Aqueous extracts collected with PILS	Direct infusion ESI (±) Orbitrap	60 000	Utility of a PILS-ESI/HR-MS approach for the molecular level analysis of WSOC constituents of laboratory aerosols and BBA
Gao et al., 2010[51]	α- and β-pinene/O_3 SOA	Solvent extraction: CH_3CN H_2O	Direct infusion nanospray ESI (±) FT-ICR (7 T)	100 000	Analysis of hundreds of products common to a range of SOA mass loadings; MS^n and LCMS analyses of molecular structures
Chang-Graham et al., 2010[26]	Biomass burning aerosols (BBA)	Aqueous extracts collected with PILS	Direct infusion ESI (+) Orbitrap	60 000	Analysis of elemental composition of individual species; identification of nitrogen, sulfur, phosphorous and metal-containing compounds in BBA samples.
Bones et al., 2010[52]	d-limonene/O_3 SOA; fresh *versus* aged with NH_3 (g), NH_4^+ (aq) samples	Solvent extraction: CH_3CN	LC-ESI (+) Orbitrap	60 000	Application of a LC-UV/Vis-ESI-MS detection for analysis of light-absorbing species in aged SOA; MS^n analysis of molecular structures
Schmitt-Kopplin et al., 2010[53]	Samples of ambient aerosols from rural sites in Hungary and Canada	Extraction in H_2O following by desalting	Direct infusion ESI (−) FT-ICR (12 T)	450 000–600 000	Observation of S- and N-containing organic compounds; new mechanism for the formation of "CHOS" compounds *via* a sulfuric acid-carbonyl reaction; parallel analysis with NMR

majority of the HR-MS studies covered in this paper have been conducted over the last three years, and we predict that the number of new applications of HR-MS to OA analysis will continue growing in the next few years. Here we provide an overview of the previously reported studies and discuss further developments and research directions in this exciting and rapidly developing area.

2. Methodology

High-resolution mass spectrometers

Mass accuracy, mass resolving power, sensitivity, dynamic range, and tandem mass spectrometry (MS^n) capabilities of a mass spectrometer are essential for characterization of individual organic compounds in complex mixtures of environmental samples.[54,55] Mass accuracy is defined as the m/z (mass-to-charge) measurement error and usually expressed in parts per million (ppm). For example, the mass measurement error of 0.001 m/z for a singly charged ion at m/z 500 corresponds to mass accuracy of 2 ppm. Mass resolving power is defined as the ratio of the peak position to its full width at half maximum, $R = m/\Delta m$. Mass accuracy reflects the difference between the measured m/z of the separated peak and the exact m/z calculated based on the elemental composition of the molecule, while R determines the ability of the instrument to separate two adjacent peaks on the m/z scale.

Several types of mass spectrometers are well-suited for complex mixture analysis; the selection of the instrument is determined by the specific application. Hybrid quadrupole time-of-flight (QTOF) mass spectrometers are characterized by very high sensitivity and dynamic range (the intensity ratio of the most abundant peak to the smallest peak in the spectrum). State-of-the-art QTOF instruments are capable of acquiring spectra with R = 20 000 and mass accuracy of 5–10 ppm at *ca.* 20 Hz repetition rate.[56] Higher mass resolution is often obtained at the expense of dynamic range and acquisition rate. For example, mass resolving power of R = 100 000 (at m/z 400) and mass accuracy of <2 ppm is obtained using an LTQ (linear ion trap)/Orbitrap instrument,[57,58] with much longer acquisition time

(1.9 s scan^{-1}) and lower dynamic range compared to QTOF. More recently, a new design of the Orbitrap analyzer has been reported, which provides R = 350 000 at m/z 524.[59]

Fourier transform ion cyclotron resonance mass spectrometry (FT-ICR MS) currently provides the highest mass resolution and mass accuracy of all existing MS technologies.[60,61] A resolving power of R = 200 000 (at m/z 400) and mass accuracy of 300 ppb were obtained using a 14.5 Tesla FT-ICR instrument and broadband acquisition at greater than one spectrum per second.[62] Much higher resolution can be achieved in FT-ICR for selected cases. For example, a record resolution of R = 3 300 000 was reported using peptide ions differing only by 0.00045 Da,[63] which is smaller than the mass of an electron (0.00055 Da)!

It should be noted that the mass resolving power of the LTQ/Orbitrap is inversely proportional to the square root of m/z[64] while that of FT-ICR instruments is inversely proportional to m/z.[65] In contrast, recently introduced ultrahigh resolution QTOF instruments are capable of acquiring mass spectra with R > 30 000 and mass accuracy of <2 ppm over a broad range of m/z values at a scan rate of 20 spectra s^{-1}.[66] As a result, QTOF instruments may outperform LTQ/Orbitrap and FT-ICR instruments for the analysis of high-MW ions (m/z > 2000).

Many studies have demonstrated that high mass resolving power and mass accuracy are needed to resolve and unambiguously identify thousands of compounds in petroleum, DOM, and aerosol samples using HR-MS. Many isobaric peaks (peaks with the same nominal mass) are typically observed for these complex samples. Fig. 1 illustrates the advantages of high resolving power for the analysis of OA samples. Fig. 1(a) shows an electrospray ionization (ESI) mass spectrum of SOA produced from an ozone-initiated oxidation of isoprene recorded at $R \sim 100\,000$. At this mass resolving power, four individual peaks around m/z 251 have been resolved and unambiguously assigned to $C_{10}H_{12}O_6Na^+$ (m/z 251.0534), $C_{11}H_{16}O_5Na^+$ (m/z 251.0900), $C_{10}H_{20}O_4Na^+$ (m/z 251.1263), and $C_{19}H_{23}^+$ (m/z 251.1794) as shown in Fig. 1(b). If the same mass spectrum was recorded at R = 5000 as illustrated in Fig. 1(c), all these peaks would be merged together into a single peak making the assignment ambiguous.

Substantially more complex spectra are observed for field-collected environmental samples. Furthermore, the spectral complexity often increases with increasing m/z. For example, in a study reported by Marshall and co-workers more than 11 000 peaks were resolved in an FT-ICR mass spectrum of a sample of South American crude oil acquired with average mass resolving power of 350 000 for m/z from 225 to 1000.[67] Detailed analysis of the spectrum revealed that the number of isobaric peaks increased from 12 peaks at nominal m/z 406 to 24 peaks at nominal m/z 588. Accurate mass measurement (<1 ppm) enabled unambiguous assignment of more than 75% peaks. Similar complexity was reported for DOM samples[68] and rural SOA samples.[53] These examples clearly illustrate the need for high resolving power for detailed chemical characterization of complex environmental samples.

Although accurate mass determination is essential for assigning elemental formulae to OA constituents, structural characterization of molecules cannot be performed without using additional tools, such as tandem mass spectrometry (MS^n). The MS^n experiment involves mass selection of the ion of interest in the first MS stage and excitation of the ion, followed by dissociation and mass analysis of the resulting fragments in the subsequent MS stages (n = 2, 3,...). The original structure of the precursor ion is then reconstructed based on the observed MS^n fragmentation pattern. Collision-induced dissociation (CID) is a widely used technique for the activation of complex ions in mass spectrometry through multiple collisions with a bath gas.[69,70] However, because of

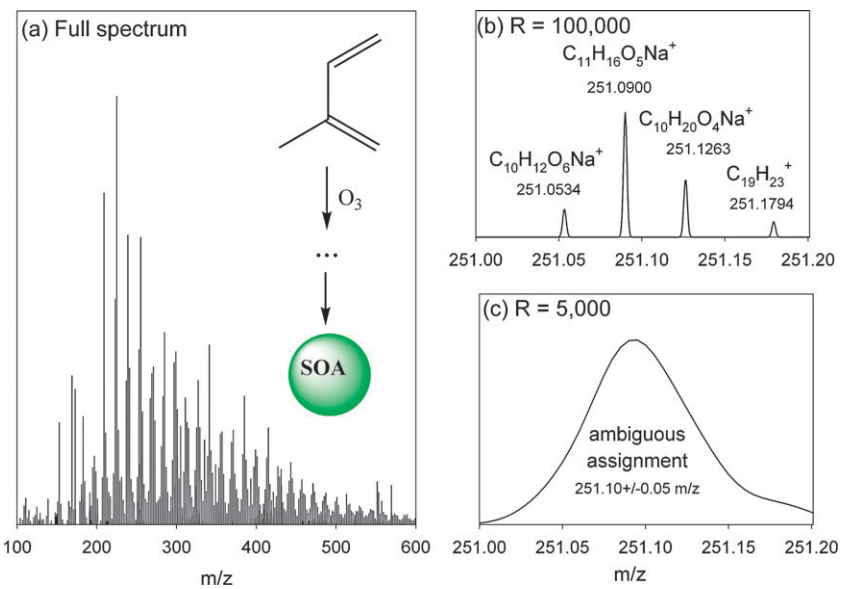

Fig. 1 A positive ion mode ESI-MS stick spectrum of isoprene/O_3 SOA (panel (a)). Panel (b) zooms in on peaks near m/z 251 recorded at the Orbitrap resolving power of R = 100 000. Panel (c) shows how the same mass range would look like if recorded at a typical resolving power of a reflection-TOF instrument R = 5000.

 This journal is © the Owner Societies 2011

the competition between ion activation and dissociation, slow stepwise energy deposition in CID experiments often results in discrimination against higher-energy dissociation pathways.[71] As a result, structure-specific fragments may be strongly suppressed or completely eliminated in multiple-collision CID. Alternative ion activation techniques suitable for MS/MS of singly charged ions include higher-energy CID in quadrupoles and linear ion traps,[72,73] surface-induced dissociation,[69,74,75] and photodissociation[76] using laser-induced excitation.

Ionization methods

A variety of soft ionization techniques in mass spectrometry may be used to generate ions of OA constituents. Traditional soft ionization methods including electrospray ionization (ESI),[77] atmospheric pressure chemical ionization (APCI),[78] and atmospheric pressure photoionization (APPI)[79] require direct collection of OA into liquid or extraction of filtered OA samples into appropriate solvents. Matrix-assisted laser desorption ionization (MALDI)[80] may be used for the analysis of samples collected on substrates but require application of a matrix for improved ionization efficiency, while ambient surface ionization techniques[81] enable analysis of analytes deposited on substrates without any sample preparation.

OA samples extracted into solvents may be analyzed using a range of ionization methods that are commonly available on commercial mass spectrometers. ESI is by far the most popular ionization technique for liquid samples.[82] In ESI, the analyte solution is dispersed into a mist of highly charged droplets produced at the end of a thin capillary to which a high voltage is applied (Fig. 2(a)). The droplets are transferred into the inlet of a mass spectrometer, where they undergo desolvation resulting in the formation of analyte ions. Polar organic solvents such as water, acetonitrile and methanol are typically used in ESI-MS experiments. Droplet desolvation is more efficient for solvents with lower surface tension. As a result, low ESI signals are often obtained when pure water is used as a solvent. Positive mode ESI spectra typically contain protonated molecules, $[M + H]^+$ or molecules cationized on metals. For aerosol samples, cationization on sodium is a common process resulting in the presence of $[M + Na]^+$ ions in mass spectra.[30] The ability of a molecule to generate $[M + H]^+$ or $[M + Na]^+$ ions is determined by its proton affinity and its ability to bind sodium cation. As a result, molecules with low proton affinities and low Na^+ binding energies cannot be ionized using ESI. For example, hydrocarbons, aliphatic aldehydes, and polycyclic aromatic hydrocarbons (PAHs) are rarely observed in ESI spectra, which can be a disadvantage in the analysis of POA samples. Negative ESI signal is dominated by deprotonated molecules, $[M - H]^-$. Because gas phase acidities are *ca.* 100 kcal mol^{-1} higher than proton affinities, deprotonation is usually less efficient than the formation of $[M + H]^+$ ions. However, ESI spectra in the negative mode often have fewer peaks and are therefore easier to interpret than spectra obtained in the positive mode.

In APCI and APPI the analyte is first evaporated and subsequently ionized using corona discharge (APCI) or 10 eV photons emitted by a krypton discharge lamp (APPI). The ionization takes place by multi-step gas-phase reactions. While ESI is ideally suited for the analysis of polar analytes, less polar molecules can be ionized using APCI, and APPI can generate ions of low-polarity species.[83] For example, APPI can be used for the analysis of lipids and polycyclic aromatic hydrocarbons that cannot be ionized using ESI. Both APCI and APPI typically produce $[M + H]^+$ ions and yield spectra that are easy to interpret. However, ionization of molecules of low proton affinity is strongly suppressed in both APCI and APPI. In addition, both techniques utilize very high flow rates of sample solutions and hence consume relatively large amounts of material per spectrum, which is not practical for the analysis of lean OA samples.

MALDI has been used both for characterization of OA generated in a smog chamber[27,84] and for analysis of field-collected samples.[27] Tolocka *et al.* observed similar oligomer distributions for SOA produced by ozonolysis of α-pinene using ESI and MALDI.[27] While MALDI is available on most commercial mass spectrometers and provides a convenient approach for the analysis of OA, it suffers from several limitations. First, matrix-related peaks dominate the signal in the low-mass range ($m/z < 250$) making it difficult to detect low-MW constituents of OA. In addition, the observed signal intensities show a significant variation with changes in the laser power, sample preparation, and sample-to-matrix ratio.

A variety of atmospheric pressure surface ionization techniques,[81,85–88] which enable rapid and sensitive characterization of samples on substrates without sample preparation, have been developed since the initial report by Cooks and co-workers in 2004.[89] These include desorption electrospray ionization (DESI),[81,89,90] in which ions are formed during collisions of electrically charged droplets with the substrate (Fig. 2(b)); direct analysis in real time (DART),[91] which utilizes a plasma of excited-state atoms and ions for simultaneous desorption and ionization of molecules from the surface of a sample; desorption atmospheric pressure chemical ionization (DAPCI);[92] electrospray-assisted laser desorption and ionization (ELDI);[93] ionization using low-temperature plasma;[94] atmospheric solids analysis probe (ASAP),[95] which relies on thermal desorption/chemical ionization of solid analytes, and a number of other hyphenated techniques.[96–98] Despite their widespread use in a variety of analytical applications, studies utilizing these methods for analysis of atmospheric aerosols are still scarce.

DESI-MS has been used for rapid quantitative detection of carboxylic acids[99] and polycyclic aromatic hydrocarbons[100] in samples of particulate matter and for characterization of aging products in laboratory-generated OA samples.[45] Because of the short residence time of analyte molecules in the solvent, DESI preserves chemically labile components of OA. However, it is often difficult to get a stable signal in DESI-MS experiments. Other ambient ionization techniques may be used for the analysis of aerosol samples collected on substrates. For example, atmospheric solids analysis probe mass spectrometry (ASAP-MS), in which the sample is thermally desorbed by a heated stream of N_2 and ionized using APCI has been utilized for analysis of SOA formed in laboratory studies and samples collected in forested and suburban areas.[101]

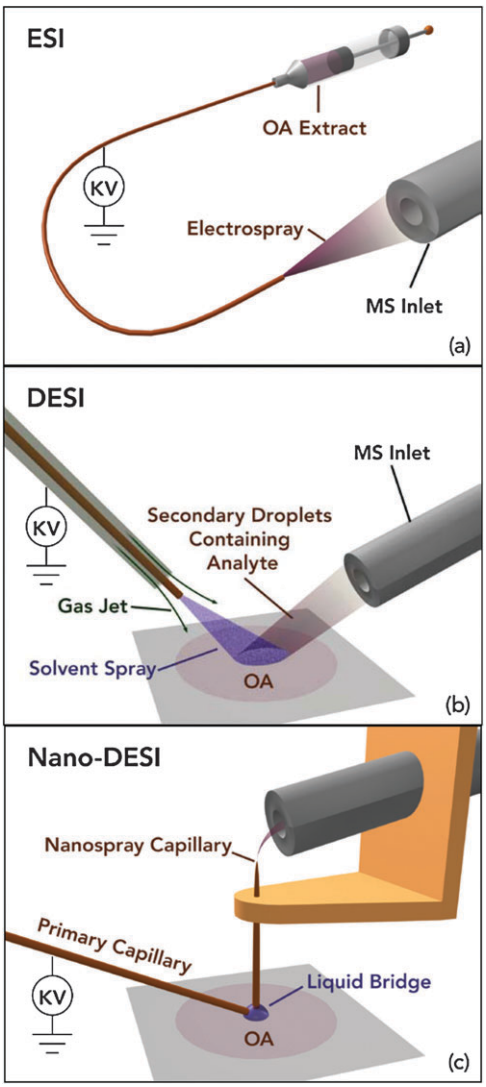

Fig. 2 Schematics of the sample introduction and ionization setups used for the analysis of organic aerosol (OA) samples: (a) direct infusion electrospray ionization (ESI); (b) desorption electrospray ionization (DESI);[45] (c) nanospray DESI. Reproduced from ref. 102.

Nanospray desorption electrospray ionization (nano-DESI)[102] is a new ambient ionization technique that has been recently applied to characterization of laboratory-generated and field-collected aerosol samples.[48] Similarly to other ambient surface ionization techniques, nano-DESI enables fast and efficient characterization of OA collected on substrates without sample preparation. In nano-DESI, the analyte is desorbed into a solvent bridge formed between two capillaries and the sample surface (Fig. 2(c)). This approach eliminates transport of the analyte on the surface, reduces the rate of the analyte consumption, and provides a stable signal for extended periods of time necessary for MS^n analysis. High-quality HR-MS spectra both for laboratory-generated and field-collected OA can be obtained with nano-DESI using only a small amount of material (<10 ng),[48] a significant benefit when analyzing leaner OA samples from remote environments. Similarly to DESI, nano-DESI enables the efficient detection of chemically labile compounds in OA because of the short solvent-analyte interaction time.

Data analysis

A variety of tools have been developed to aid the analysis of hundreds of features observed in high-resolution mass spectra of OA and related environmental organic mixtures. Kendrick transformation[103–105] is often used to identify homologous compounds differing only by a number of base units. In this approach the experimental m/z value is normalized to the nominal mass of a chemical group used as a basis for this analysis (*e.g.*, CH_2, O, CH_2O, *etc.*). For example, for the CH_2-based diagram the Kendrick mass (KM_{CH2}) is calculated by re-normalizing the IUPAC mass scale to the exact mass of the $^{12}CH_2$ group (*i.e.* 14.0156 amu) using eqn (1).

$$\mathrm{KM} = \text{observed mass} \times (\text{nominal mass of } CH_2 = 14)/(\text{exact mass of } CH_2) \quad (1)$$

The Kendrick mass defect (KMD) is calculated as the difference between the nominal mass (NM), defined as KM rounded to the nearest integer, and KM using eqn (2):

$$\mathrm{KMD} = \mathrm{NM} - \mathrm{KM} \quad (2)$$

The advantage of Kendrick analysis is that homologous compounds differing only by the number of base units (CH_2 in this example) have identical KMD values. When the KMD is plotted *versus* the mass-to-charge ratio of a compound, homologous series fall on horizontal lines and are clearly distinguishable.[103] Assignment of the elemental composition of one compound in the homologous series automatically identifies all remaining peaks in the series. Fig. 3(a) shows CH_2-based Kendrick plots for neutral species identified in positive and negative mode ESI-MS spectra of isoprene SOA. Homologous CH_2-series of up to $n = 10$ members were observed in these spectra. The insert in Fig. 3(a) shows two adjacent series; such series are readily identified in a complex spectrum using Kendrick analysis.

However, different homologous series may have similar values of KMD. As a result, additional pre-sorting of the data capable of separating Kendrick series with similar values of KMD is often necessary. One possible pre-sorting parameter is a nominal mass index, z*,[106] defined for the CH_2-based Kendrick analysis by eqn (3). It can assume values between −1 and −14. Members of a given CH_2 homologous series have the same z* and KMD values.

$$z^* = \text{modulo } (\mathrm{NM}/14) - 14 \quad (3)$$

Pre-sorting of the Kendrick series based on the z* index has been used for classification of compounds in complex high-resolution mass spectra of crude oil[106] and fulvic acids.[107]

Molecular formulae of compounds containing elements which possess several isotopes are calculated using the most abundant isotope for each element. Mathematically correct formulae can be assigned by considering all possible combinations of atoms consistent with the measured accurate mass of the ion. However, such unconstrained search often yields chemically unreasonable and redundant assignments even when the data are acquired at very high resolution. For example,

 This journal is © the Owner Societies 2011

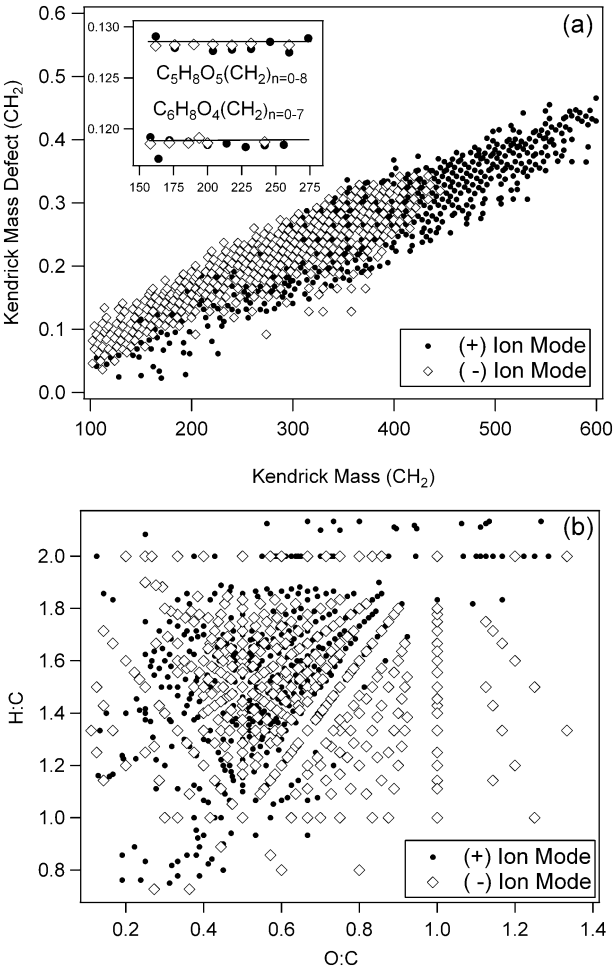

Fig. 3 Examples of a CH_2-Kendrick diagram (a) and a van Krevelen diagram (b) for an isoprene/O_3 SOA sample. Plots were generated from experimental data reported in ref. 44. The ± 0.001 m/z deviations between the measured and expected Kendrick mass defect values are typical for the Orbitrap MS.

an unconstrained search for $m/z = 200.0000$ returns an unlikely formula of $C_{13}N_2O$ as the closest match. The list of elemental formulae obtained from the unconstrained search must therefore be filtered based on a number of rules including the degree of unsaturation, parity, valence rules, isotopic patterns, and H/C or O/C ratios.[108]

The degree of unsaturation or the ring and double bond equivalent (DBE) can be calculated using eqn (4):[109]

$$\mathrm{DBE} = x + 1 + 0.5(z - y) \quad (4)$$

where x is the number of tetravalent atoms (C, Si), y is the number of monovalent atoms (H, Cl, Br), and z is the number of trivalent atoms (N,P) in the molecule. For example, for a neutral molecule $C_{13}H_{15}NO_4$ observed in a positive ESI spectrum as $[C_{13}H_{15}NO_4 + H]^+$, the value of DBE is 7 ($x = 13$, $y = 15$, $z = 1$). Non-integer values of DBE are obtained for ions and radicals while closed-shell neutral molecules have integer DBE values. DBE can be used to restrict the search to charged or neutral species and to eliminate molecules with unreasonably high or low number of rings and double bonds. However, complications arise because certain atmospherically relevant elements may have multiple valence states, for example the valence of N is 3 in amines and 5 in nitric acid esters (alkyl nitrates). Valence of S is 2 in sulfides but it increases to 6 in sulfuric acid esters. In such cases, where the valence state cannot be determined *a priori*, calculated DBE values need to be considered with caution.

Another simple filter for the formula assignment is based on the well-known nitrogen rule. The nitrogen rule derives from the fact that chemical elements with even nominal mass have an even valence, while elements with odd mass have an odd valence, with the exception of nitrogen, which has a nominal mass of 14 and a valence of 3 or 5. As a result, all organic compounds of the general formula $C_cH_hO_oS_sN_nP_p$ have a nominal mass which is an even number when the number of nitrogen atoms (n) is even ($n = 0,2,\ldots$) and an odd number when n is odd ($n = 1,3,\ldots$). ESI ionization inverts this parity because a positive mode ESI results in the addition of H^+ ($m/z = \mathrm{MW} + 1$) or Na^+ ($m/z = \mathrm{MW} + 23$) to the molecule while in the negative mode most ions correspond to deprotonated species ($m/z = \mathrm{MW} - 1$). It follows, that ions produced in ESI have an even nominal mass only when the molecule contains an odd number of nitrogen atoms. Isotope distributions may complicate the matter: ions containing no nitrogen and an odd number of ^{13}C and/or D atoms also appear at even nominal masses in the ESI spectra. However, such species do not normally pose a problem because their peaks can be fully resolved from the peaks corresponding to N-containing ions at moderately high mass resolving power. In addition, the peak intensities of isotopically substituted ions are constrained by the low natural abundance of ^{13}C and D. If a peak appears at an even nominal mass, and its intensity exceeds that expected for the isotopically substituted ions, it can be safely assumed that it corresponds to a N-containing ion.

The redundancy in formula assignment is dramatically reduced when the search is constrained based on the valence of each element. The Molecular Formula Calculator (http://magnet.fsu.edu/~midas/) developed at the National High Field Magnet Laboratory is a freeware program capable of formula assignment based on valence rules. However, redundant assignments are often obtained even when the valences are constrained. Additional constraints can be imposed by comparing the calculated isotopic pattern for the candidate formula with the isotopic pattern observed experimentally. This constraint is particularly useful for assigning formulae for chlorine-, sulfur- and metal-containing compounds because they often possess distinct isotopic distributions. Finally, the candidate formulae can be filtered based on the H/C ratio and the heteroatom ratio. For example, analysis of 45 000 formulae in the Wiley spectral database showed that 99.7% compounds have the H/C ratio in the range from 0.2 to 3.1, N/C ratio in the range of 0–1.3, O/C ratio in the range of 0–1.2.[108] This information can be used to eliminate some unreasonable formula assignments.

Data visualization

Several visualization approaches are commonly used to facilitate interpretation of the HR-MS data.[105,110] The

van Krevelen diagram (VK) is constructed by plotting H/C *versus* O/C elemental ratios.[68] An example of a VK diagram obtained for the isoprene SOA sample is shown in Fig. 3(b). Such a representation is attractive to atmospheric aerosol chemists because it provides direct visualization of the range of O/C ratios in the molecular OA constituents. The average O/C ratio is a convenient measure of the degree of oxidation and aging in organic aerosols.[111,112] Additional dimensionality is added to VK diagrams by either scaling the size of data points with the intensity of the corresponding peak or by plotting them as heat maps.[105] In addition, three-dimensional VK plots may be generated using the N/C ratio[113] or the DBE[44] as a third variable, which enables better visual separation between different classes of molecules present in complex samples. Finally, data visualization often relies on graphs showing the variation in the DBE,[39,42] the carbon number,[110] or the H/C and O/C ratios[48] as a function of the experimental m/z values.

3. Understanding molecular chemistry of OA using HR-MS analysis

Laboratory studies of model SOA systems

Laboratory studies of processes leading to the formation of organic aerosols are routinely conducted in "smog chambers" because they offer control over the reagent concentrations, humidity, temperature, and UV illumination levels. Smog chambers range from a few cubic meters to a few hundred cubic meters in volume. They are typically made of inert, UV transparent materials such as Teflon film. For example, our groups are using a 5 m^3 Teflon chamber surrounded by 40 UV-B lamps for photochemical generation of OH from photolysis of H_2O_2 and HONO (Fig. 4). Other common atmospheric oxidants such as O_3 and NO_3 may be added to the chamber directly through side ports, along with the precursor VOC of interest. OA formation may be studied at different O_3 or NO_x concentrations and humidity levels, in darkness or in the presence of UV radiation. The chamber is connected to a suite of instruments that control and monitor the reaction conditions: zero-air generator, NO_y monitor, O_3 monitor, scanning mobility particle sizer, chemical ionization mass spectrometer,[114] time-of-flight aerosol mass spectrometer,[17] proton-transfer-reaction time-of-flight mass spectrometer.[115] The resulting SOA is collected using traditional filters, a multi-orifice uniform-deposit impactor, particle-into-liquid samplers (PILS),[116] or other aerosol collectors. Suitable denuders may be inserted between the collector and the chamber to remove gaseous species.

HR-MS analysis has provided a qualitatively different way of discovering new chemical processes leading to or occurring in OA in smog chamber studies. Arguably the greatest impact of HR-MS has been on our understanding of the composition and formation of "oligomers", molecules composed of two or more first generation products of VOC oxidation bound together by esterification, hemiacetal formation, aldol condensation, and other reactions. Oligomerization reactions are important because they convert volatile molecules into higher-MW products of lower volatility. As a result, molecules that would otherwise be too volatile to partition into the particle phase in the monomeric form are trapped in the condensed phase. The complexity of oligomeric species prevented their molecular characterization until HR-MS methods came along.

Tolocka *et al.*[27] were the first to observe oligomers in SOA from ozone oxidation of α-pinene. They used FT-ICR to observe "dimer", "trimer", and "tetramer" compounds corresponding to molecules composed of two, three, and four first-generation α-pinene oxidation products, respectively. Detailed analysis of the assigned chemical formulae and MS^n spectra showed that oligomers are produced by acid-catalyzed aldol condensation and *gem*-diol formation. Reinhardt *et al.*[29] examined the α-pinene SOA oligomers at an even higher mass resolving power. By using the data analysis and visualization methods discussed in the previous section, they examined the distribution of the m/z differences between the observed peaks and identified $C_{10}H_{16}O_6$ and several other monomers with 6–12 C atoms and 0–7 O atoms as the most common oligomer building blocks. These and subsequent studies[27,29,37,40,49,51] have provided the most comprehensive list of molecular constituents in α-pinene SOA.

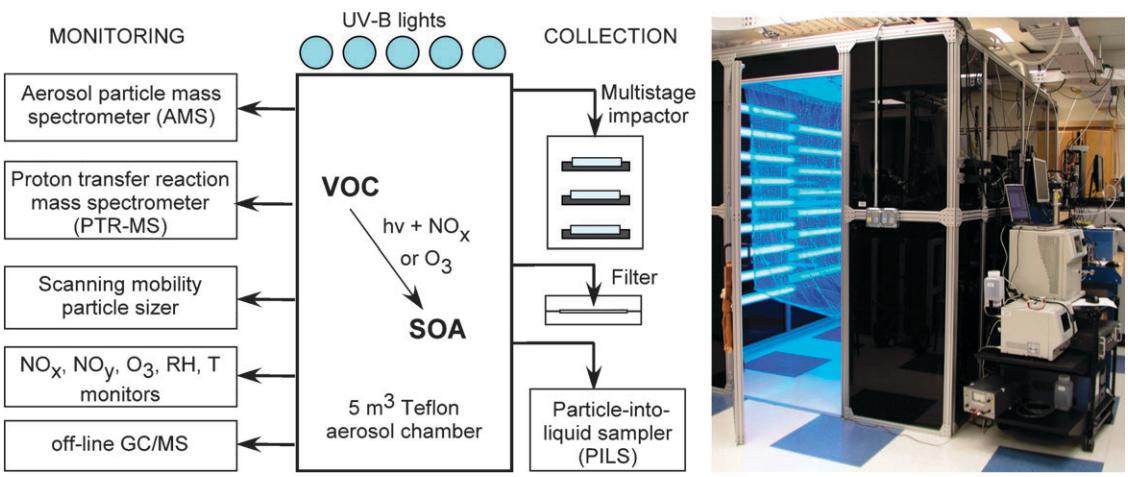

Fig. 4 A schematic diagram and a photograph of the UCI aerosol chamber used for generation of model SOA. The particles are generated in a Teflon chamber, collected with filters, impactors, or a particle into liquid sampler (PILS), and subsequently analyzed with HR MS.

 This journal is © the Owner Societies 2011

Our groups have investigated different aspects of chemistry of SOA formed by ozone-initiated oxidation of d-limonene[30,31,39,45,50]—an important aerosol precursor in both indoor and outdoor environments.[117] We found that OA produced by ozonolysis of d-limonene contain hundreds of different products including a large number of oligomeric compounds.[30] Time-resolved collection of size-selected SOA samples revealed that oligomers form within minutes of mixing ozone and d-limonene, and that the composition of SOA undergoes slow changes as a result of heterogeneous oxidation by ozone.[39] The observed mass spectra were surprisingly insensitive to the reaction conditions such as reactant concentration, humidity, presence of UV radiation, and addition of OH scavengers.[39] The observed distribution of compounds in limonene SOA showed that oligomerization is driven by reactions of carbonyl oxides (Criegee intermediates) with various first-generation monomeric products of oxidation.[30] We searched for evidence of oligomerization occurring *via* hemiacetal formation (carbonyl + hydroxy group), esterification (carboxyl + hydroxy with loss of water), and aldol condensation (carbonyl + carbonyl with loss of water). However, the observed distribution of DBE values between monomers (average DBE = 3), dimers (average DBE = 5), trimers (average DBE = 7), and tetramers (average DBE = 7) showed that esterification and aldol condensation are insignificant in limonene SOA, even under low relative humidity conditions that promote condensation processes.

Nguyen *et al.*[44] examined SOA from ozone-initiated oxidation of isoprene, C_5H_8, the most abundant biogenic hydrocarbon after methane.[118] Similar to the α-pinene and d-limonene SOA, mass spectra of isoprene SOA were highly complex, with more than 1000 assignable peaks appearing in the positive and negative ion mode ESI spectra (Fig. 1(a)). The stark contrast between the molecular weights of isoprene (68 amu) and observed condensable reaction products (100–600 amu) suggested extensive oligomerization. Indeed, the absolute majority of the detected peaks corresponded to previously-uncharacterized, highly-oxidized, oligomeric compounds, with an average O/C molar ratio of 0.6. Detailed analysis of the identified compounds revealed the potential importance of formaldehyde in the SOA growth: the most frequently observed difference between the observed peaks corresponded to CH_2O. This observation supported the hypothesis of SOA growth *via* accretion of small carbonyls.[9,119–121]

Oligomeric products with high DBE and low O/C values corresponding to molecules with multiple unsaturated C=C bonds were also detected (*e.g.*, $C_{19}H_{22}$ with DBE = 9 appearing in Fig. 1(b)). These molecules occupy the bottom left corner of the VK diagram in Fig. 3(b). Similar products with high DBE and low O/C were detected in the ozonolysis of α-pinene.[40] Formation of such products under the high oxidizing environment of these experiments is surprising. Clearly several competing oligomerization mechanisms (free radical polymerization; reaction of Criegee intermediates with acids, alcohols, and carbonyls; hemiacetal formation, *etc.*) must be operating in reactions of terpenes with ozone.

Perhaps the most impressive example of new chemistry revealed by an HR-MS method comes from our recent investigation of reactions between limonene SOA compounds and reduced nitrogen compounds.[45] We previously observed that such reactions produce light-absorbing compounds in SOA on atmospherically relevant time scales.[122] The SOA sample or its aqueous extract turns brown when exposed to trace amounts of ammonia (even small amounts of NH_3 found in typical indoor environments are sufficient to drive the reaction). Brown aerosols have a significant effect on the climate because they absorb solar radiation instead of scattering it back into space.[123] Chemical processes leading to the formation of chromophores are therefore relevant for the accurate prediction of direct effects of OA on the climate. UV/Vis, FTIR, NMR and 3D-fluorescence spectroscopy measurements suggested that the chromophores responsible for light absorption in the aged limonene SOA are nitrogen-containing molecules, most likely conjugated imines formed in ammonia–carbonyl reactions.[122] To prove this hypothesis we prepared "fresh" d-limonene SOA samples, exposed them to sub-ppm concentrations of gaseous NH_3 in humid air, and examined the aged, brown SOA using DESI HR-MS.[45] Detailed analysis of the aged SOA samples revealed the presence of a significant number of nitrogen-containing products. The reaction mechanism that rationalizes the results of the DESI HR-MS experiments is shown in Fig. 5. We found that a number of carbonyl compounds in SOA underwent a >C=O to >C=NH conversion upon exposure to ammonia, evidenced by a characteristic peak shift of $\Delta m/z = -0.9840$ (Fig. 5(a)). The resulting imines readily reacted with additional carbonyl compounds forming substituted imines as shown in Fig. 5(b). An intramolecular version of the same reaction leading to heterocyclic compounds (Fig. 5(c)) was also observed.[45,52] These types of reactions may serve as a source of nitrogen-containing compounds in aerosols, especially in areas where anthropogenic NH_3 emissions mix with anthropogenic or biogenic SOA. A recent paper by Wang *et al.*[124] reported N-containing compounds consistent with this formation mechanism in urban air.

HR-MS methods find increasing use in the estimation of the average elemental and mass ratios between H, O, C, and N in environmental samples. As discussed in ref. 111 and 112, such ratios are difficult to obtain for OA by more traditional analytical techniques. For example, commercial CHNO analyzers such as Perkin-Elmer 2400-series instruments typically require milligram quantities of sample, an amount that is hard to collect for atmospheric aerosols. In contrast mass spectrometry methods are capable of providing such information using only nanograms of material. The conventional approach relies on thermal decomposition of the sample in an oxidizing environment and measurement of evolved CO_2 to quantify the total mass of organic carbon (OC). The total organic mass (OM) is then estimated by multiplying the measured OC value by an empirical OM/OC ratio, which ranges from about 1.4 to 2.3 depending on the type of organics present in OA.[125,126] In the case of fully soluble OA samples, the OM/OC ratio can be reasonably

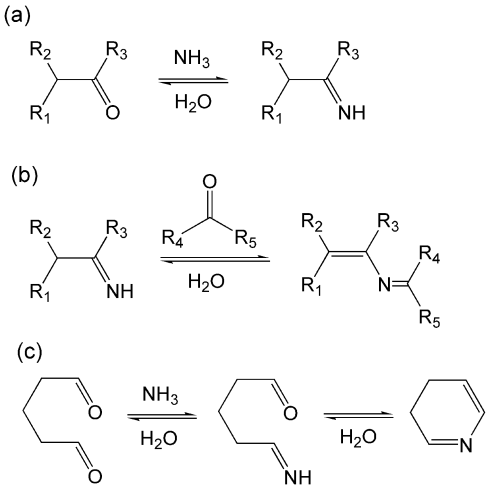

Fig. 5 Reactions of NH_3 with carbonyl species in OA inferred from DESI HR-MS experiments.[45] (a) Carbonyl-to-imine conversion with a characteristic peak shift of −0.9840 m/z. (b) Intermolecular condensation of the resulting imine with another carbonyl leading to a substituted imine. (c) Intramolecular conversion of 1,5-dicarbonyls into a heterocyclic imine with a characteristic peak shift of −18.9946 m/z.

estimated from the HR-MS data using the following equations:

$$\langle O/C \rangle = \sum_i x_i o_i \Big/ \sum_i x_i c_i \tag{5}$$

$$\langle H/C \rangle = \sum_i x_i h_i \Big/ \sum_i x_i c_i \tag{6}$$

$$\frac{OM}{OC} = 1 + \frac{16}{12}\langle O/C \rangle + \frac{1}{12}\langle H/C \rangle \tag{7}$$

where h_i, c_i, and o_i are the numbers of H, C, and O atoms in each compound, and x_i is a weight factor. We have found that the average elemental and OM/OC ratios for model SOA are remarkably insensitive to the exact nature of the weighing factors.[39,44] For example, taking x_i as normalized peak intensities in the mass spectrum or setting all x_i to 1 produces nearly identical results for laboratory-generated aerosols. In case of the isoprene SOA (Fig. 3), the average O/C ratio is about 0.60 and the corresponding OM/OC ratio is about 1.9.[44] The applicability of this approach to the field OA samples is yet to be verified.

Chemical characterization of ambient aerosol samples

A number of recent field studies have employed HR-MS analysis for comprehensive assessment of molecular composition of OA and its atmospheric chemistry. Ambient aerosols contain a substantially more complex mixture of organic species with less predictable composition compared to laboratory generated SOA discussed above. For instance, one of the most important sources of OA in the atmosphere is burning of biomass in naturally occurring and prescribed forest fires.[127] Identifying the chemical composition of biomass burning aerosols (BBA) is necessary to understand its short- and long-term effects on air quality, climate and human health. A number of recent studies have employed HR-MS coupled with soft ionization techniques such as ESI and nano-DESI for the structural characterization of molecules in the complex mixtures of BBA samples.[26,41,42,48,50] Fig. 6 shows representative positive mode ESI/HR-MS spectra of three selected BBA samples collected in controlled burns of different biomass fuels materials: Southern Pine needles (SPN), Ponderosa Pine duff (PPD), Ponderosa Pine needles and sticks (PPNS).[41] Clearly, different samples yield distinctly different spectra demonstrating the utility of the HR-MS analysis for detection of characteristic markers for BBA emitted from burning different types of biomass fuels. Accurate mass measurements assisted with Kendrick analysis enabled unambiguous peak assignments to hundreds of individual organic compounds over the mass range of m/z of 100–1000. The results showed that a variety of highly oxidized oxygenated organic compounds and nitrogen-containing alkaloid compounds that have not been previously reported in the literature account for a significant fraction of BBA extracts.[41,42]

Physical and chemical properties of aerosols depend on their molecular compositions. For example, organic molecules are more likely to absorb visible light if they have a large number of double bonds and rings (=DBE).[128] In addition, hygroscopic growth factors[129] and UV/Vis absorption spectra[45,52,122] of OA may be correlated with the presence of oxygenated and nitrogen-containing organic compounds. The values of O/C, H/C, and N/C ratios are often related to specific emission sources and aging mechanisms of OA.[111,112,130,131] It follows that accurate mass measurements and assignments of molecular formulae based on ESI/HR-MS analysis offer useful data on specific types and groups of ambient OA and unique

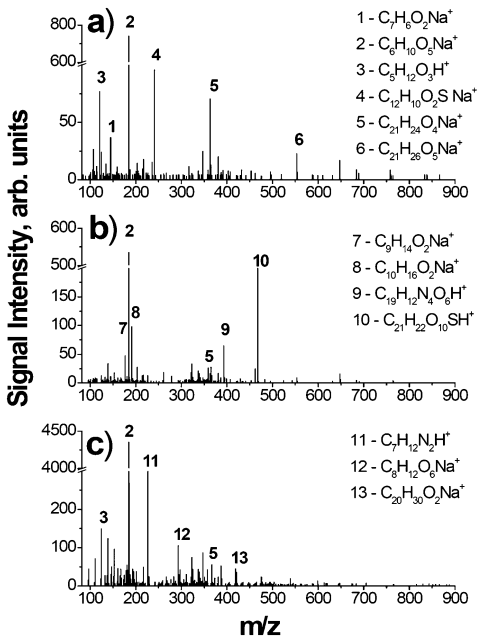

Fig. 6 Examples of high resolution positive ion mode ESI mass spectra of three different BBA samples obtained from burning of: (a) Southern Pine needles, (b) Ponderosa Pine duff, and (c) Ponderosa Pine needles and sticks. Abundant peaks are listed in the plot. Reproduced from ref. 41.

 This journal is © the Owner Societies 2011

"marker" molecules. Combined with complementary measurements of aerosol physicochemical properties, these data provide basic knowledge for improved classification of complex mixtures of OA with respect to their potential atmospheric reactivity, optical and hygroscopic properties.

Fig. 7(a) shows an H/C *vs.* N/C VK plot, and Fig. 7(b) shows a plot DBE *vs.* *m*/*z* values for various nitrogen-containing organic species detected in BBA emitted from burning of the PPNS biomass.[42] The observed N/C ratios were as high as 0.4, and DBE values reached 9 for certain N-containing families. A number of analyte molecules clearly had related structures because they formed long CH_2 Kendrick families (Fig. 7(b)).

Accurate mass assignment combined with MS^n experiments for structure determination have been successfully used in a number of studies for structural characterization of individual molecules present in complex mixtures of OA.[27,34,37,42,45,52] Fig. 8 illustrates examples of core structures of several homologous series in BBA identified using MS^n.[42] Plausible structural assignments were made based on the known fragmentation behavior of protonated molecules reported in the literature.[132] It has been demonstrated that fairly basic N-heterocyclic compounds comprise a substantial fraction of nitrogen-containing species in some of the BBA samples relevant to specific biomass fuels. Because of their high basicity, these compounds may buffer the acidity of aerosols, and thereby have an impact on the heterogeneous chemistry of particles, their hygroscopic and optical properties.

A significant fraction (30–70%) of ambient aerosol corresponds to water soluble organic carbon (WSOC) comprised of high-MW humic-like substances (HULIS) (*e.g.* ref. 133). Water soluble organic nitrogen (WSON) compounds, a subset of WSOC, are of particular interest because of their profound impact on the nitrogen concentration in aquatic and terrestrial ecosystems,[134–137] which have a significant effect on the total nitrogen cycle on Earth.[138] However, very little is known about detailed chemical composition of WSON compounds in OA, their source apportionment, and atmospheric evolution. ESI/HR-MS is the technique of choice for structural characterization of complex WSON mixtures relevant to ambient aerosols. A number of studies focused on characterization of WSON compounds in rain and fog samples,[38,43,46] aqueous extracts of ambient OA samples,[28,33] and aqueous extracts of BBA samples.[26,48,50] Altieri *et al.*[38,43] and Mazzoleni *et al.*[46] identified main groups and homologous series of oligomers, organosulfates, nitrooxy-organosulfates and a number of nitrogen-, sulfur- and mixed compound with reduced N-functionalities in rain water and fog samples. In those works elemental compositions of 500–1300 individual molecules in the *m*/*z* range of 50–500 were determined and specific organic groups were assigned. Reemtsma *et al.*[28] and Wozniak *et al.*[33] reported identification of fulvic acids along

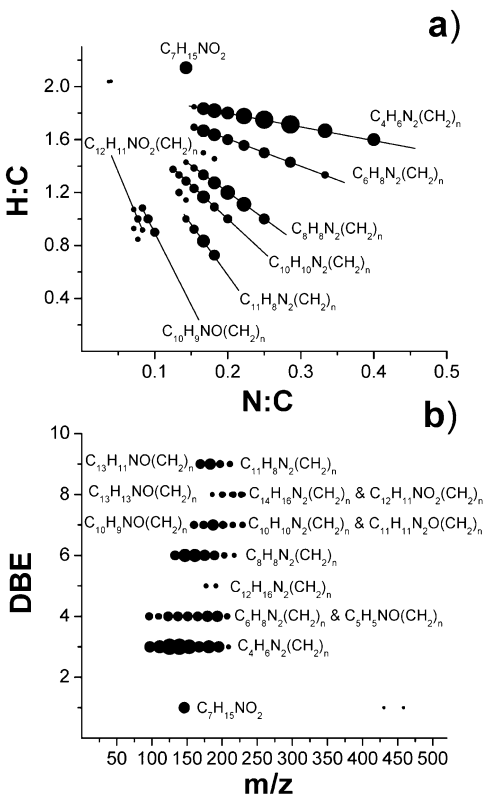

Fig. 7 (a) Van Krevelen plot for homologous series of N-containing organics detected in the PPNS sample; (b) DBE values calculated for the same series as a function of *m*/*z*. The size of the symbols is proportional to the logarithm of the peak intensity. *n* refers to the number of CH_2 groups in a given family: (n = 1–9)-$C_4H_6N_2$, (0–3,11)-C_5H_5NO, (0–7)-$C_6H_8N_2$, (0)-$C_7H_{15}NO_2$, (0–6)-$C_8H_8N_2$, (0–2)-$C_{10}H_9NO$, (0–5)-$C_{10}H_{10}N_2$, (0–3)-$C_{11}H_8N_2$, (0–3)-$C_{11}H_{11}N_2O$, (0,1)-$C_{11}H_{16}N_2$, (0–2)-$C_{12}H_{11}NO_2$, (0,1)-$C_{13}H_{11}NO$, (0,1)-$C_{13}H_{11}NO$, (0–2)-$C_{14}H_{16}N_2$. Reproduced from ref. 42.

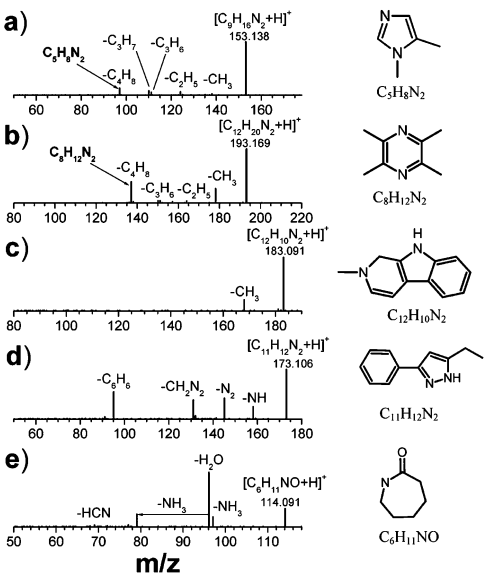

Fig. 8 Representative MS^2 spectra of nitrogen-containing compounds in BBA indicate presence of N-heterocyclic aromatic compounds. Elemental formulae in squared parentheses indicate precursor ions. Elemental formulae above fragment ions denote the corresponding loss of neutral molecules in MS^2 experiments. Elemental formulae of fragments corresponding to the stable molecular core of two major CH_2-homologous series are labeled in panels (a) and (b) and the corresponding structures are shown on the right. The proposed structures of neutral precursor molecules for spectra shown in panels (c)–(e) are displayed on the right. Reproduced from ref. 42.

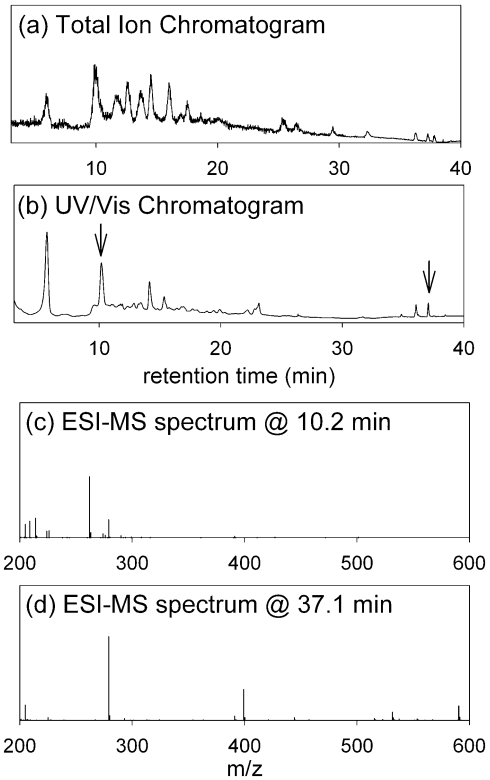

Fig. 9 Sample LC-UV/Vis-MS data for a limonene SOA sample "aged" by reaction with glycine. Total ion (a) and UV/Vis signal (300–600 nm) (b) as a function of retention time. The ESI spectra corresponding to elution at 10.2 min (c) and 37.1 min (d) are considerably simpler than the direct-injection ESI spectrum of the aged SOA sample.

with organosulfates and organonitrates in water-soluble organic fractions of atmospheric aerosols. They found that lignin-like and lipid-like compounds constitute a significant fraction of ambient aerosol collected in the areas of studies. In addition, a small fraction of WSOC compounds was classified as black carbon (BC) based on the high DBE values. Schmitt-Kopplin *et al.*[53] identified N- and S-containing organic compounds in rural aerosol samples dominated by SOA but also affected by local anthropogenic and biomass burning activities. Most recent studies reported detailed characterization of WSON compounds characteristic of BBA samples,[26,48,50] including those relevant to burning of biomass collected at military ranges.[26] The latter study reported detailed ESI/HR-MS characterization of BBA emissions from laboratory controlled burns of biomass representative of vegetation in selected U.S. military bases. The results indicated that water soluble nitrogen- and metal-containing organic compounds are ubiquitous in the BBA samples, including those with transition metals such as Cr, Mn, Fe, Ni, Cu, and Zn. It has been concluded that biomass can accumulate metal-containing species and reemit these metals through biomass burning.

4. Future directions

As illustrated above, HR-MS is a unique tool for comprehensive chemical characterization of individual molecules in ambient aerosol. In the next few years, we are likely to see both further development of HR-MS capabilities and integration of HR-MS with other methods for OA analysis. The following discussion is not intended to convey a comprehensive review of all possible future directions, but rather embraces ongoing efforts in the authors' groups focused on the development and applications of HR-MS approaches for fundamental studies of organic aerosol chemistry.

Coupling of HR-MS to separation techniques

The above discussion focused on applications of HR-MS methods that rely on direct infusion of analytes. While such methods provide useful information on the overall composition of OA, they do not always make it possible to focus on OA constituents with specific physical or chemical properties. In addition, direct HR-MS methods cannot readily distinguish structural and stereo isomers, which have the same molecular weights and similar MS/MS spectra. Coupling HR-MS with liquid chromatography (LC) may help overcome these limitations. For increased specificity, the LC-separated OA compounds may be simultaneously analyzed using additional detectors, such as a UV/Vis absorption or fluorescence detector, before the HR-MS analysis.

LC-UV/Vis-HR-MS is especially attractive for characterization of light-absorbing compounds in aerosols. Instead of analyzing the full mass spectrum one can focus on a subset of compounds that absorb at specific wavelengths. As a proof of principle, we have applied this method to brown limonene SOA aged by reduced nitrogen compounds. Fig. 9 demonstrates that the light-absorbing compounds can be successfully separated on a C18 reverse-phase LC column and detected with a UV/Vis detector. Each peak in the UV/Vis chromatogram corresponds to a unique mass spectrum. The mass spectra corresponding to the elution of the colored compounds are still complex suggesting incomplete LC separation. However, they contain 1–2 orders of magnitude fewer peaks ($\sim$10 peaks) than mass spectra of the whole sample (10^3–10^4 peaks), which significantly simplifies the assignment of the chromophores. We are currently in the process of developing tools for processing the LC-UV/Vis-HR-MS data, and applying this method to both laboratory and field samples of brown aerosols.

Advancing applications of HR-MS analysis in field studies

Understanding fundamental chemistry of atmospheric aerosols relies on integration of molecular-level insights and measurements obtained by multiple field and laboratory methods.[5,6,139] Because of the unique HR-MS capabilities highlighted throughout this manuscript, the demands on the HR-MS measurements will likely increase in future studies of aerosol chemistry. However, field deployment of FT-ICR and LTQ/Orbitrap instruments is not currently possible because of their large size, heavy weight, and substantial power requirements. Their common use in laboratory studies by broad community of aerosol researches is also hindered by their high cost and typically limited availability of instrument time managed by user facilities. Consequently, all HR-MS studies of OA and cloud/fog samples rely on appropriate

 This journal is © the Owner Societies 2011

methods of sample collection and pre-analysis storage. Most of the studies listed in Table 1 utilized time- and size-integrated samples collected over extended periods of time. Application of size-selective, and automated time-resolved sampling approaches will be practical in future laboratory and field studies focused on capturing variations in aerosol composition for specific events of interest, *i.e.*, aerosol photochemistry upon UV irradiation from aerosol chambers, field sampling during traffic rush hours, sampling from moving platforms *etc.* For instance, particle-into-liquid sampler (PILS)[116] enables continuous, time-resolved aqueous extraction and collection of aerosol WSOC constituents into a set of vials, which can be directly analyzed by the ESI/HR-MS methods.[50] The modified three-stage rotating drum impactor may be used to collect intermittent time-resolved samples of OA onto Teflon strips.[39] OA samples with better size resolution may be collected using multi-stage cascade impactors.[39]

The time necessary for sample collection is determined by the sensitivity of the specific analytical technique considered for later sample introduction and ionization. In this regard, nano-DESI approach poses an exceptional promise for sensitive analysis of very small aerosol samples. We demonstrated that this approach can be routinely used to provide high-quality HR-MS data using less than 10 ng of OA material.[48] Assuming, ambient OA concentration of 1 μg m^{-3} typical for unpolluted environments, sampling of 10 L of air is sufficient for obtaining a good-quality nano-DESI MS spectrum. A time resolved aerosol collector[140] that deposits sequential aerosol samples, each over a sampling area of ~1 mm in diameter, can provide a set of samples perfectly suitable for nano-DESI analysis, collected with the time resolution better than 10 min between two consecutive samples.

Further development of atmospheric pressure desorption ionization techniques is required for high-throughput analysis of OA samples collected on substrates. These studies should address a number of challenges in OA analysis including poor ionization of non-polar compounds, ionization of chemically labile oligomeric species without fragmentation, formation of cluster ions that interfere with the analysis of oligomers. In addition, technical advances in the development of automated loading and analysis approaches are necessary for high throughput applications and the analysis of time-resolved aerosol samples.

Future work is needed for the development and application of novel HR-MS analysis approaches coupled directly to sampling devices. These types of techniques, wherever they are practical, will eliminate possible issues of sample storage, and also will provide unique tools for kinetics and reaction mechanism studies of aerosol and cloud droplet chemistry. An innovative set of experiments was carried out by Perri *et al.*[36,47] using a low resolution ESI-MS analysis of samples continuously withdrawn from a reaction vessel containing aqueous solution of organic molecules relevant to SOA formation through cloud and fog chemistry. Elucidation of the identities and yields of aqueous-phase SOA products reported in such studies will be greatly improved if coupled to HR-MS instrumentation, especially if it is also assisted with an LC separation stage. *In situ* HR-MS analysis of ambient aerosols is another challenging task. A promising method of crossed nano-ESI and focused aerosol sprays has been recently utilized for quantitative analysis of aerosolized drugs.[141]

Specific analyte modification coupled with HR-MS analysis

Addition of reagents to the spray solvent for targeted detection and ionization of selected analyte molecules, may be used as a tool for improved characterization of functional groups in OA samples. Reactive DESI-MS experiments have been used for analysis of biomolecules, explosives, and in forensics applications,[87,142] but have not been widely employed by the aerosol chemistry community yet. Limited studies focused on reactive ESI-MS detection of aldehydes in SOA samples using Girard Reagent P[143] and methanol.[31] Fig. 10 shows characteristic fragments of positive ion mode mass spectra of d-limonene SOA reacted with methanol, and d_3-methanol solvents. Substantial differences between mass spectra of the same SOA sample extracted into methanol and d_3-methanol indicate addition of methanol to SOA compounds containing an aldehyde group. Specifically, the peak at m/z 191.1043 corresponds to a limononaldehyde SOA product,[30,31] which upon reaction with methanol and d_3-methanol yields hemiacetal products observed at m/z 223.1305 (panel a), and at m/z 226.1494 (panel b), respectively. Similar reactions were also reported for other SOA constituents containing carbonyl and carboxyl groups. Acetal formation and esterification reactions were used to estimate the relative fractions of carbonyl (>42%) and carboxylic acid (>55%) groups characteristic of the d-limonene SOA. Analogous applications of other reagents for reactive HR-MS analysis may greatly enhance our knowledge of the chemical composition of OA, with potential to describe functional groups and also estimate their chemical reactivity relevant to the atmospheric environment.

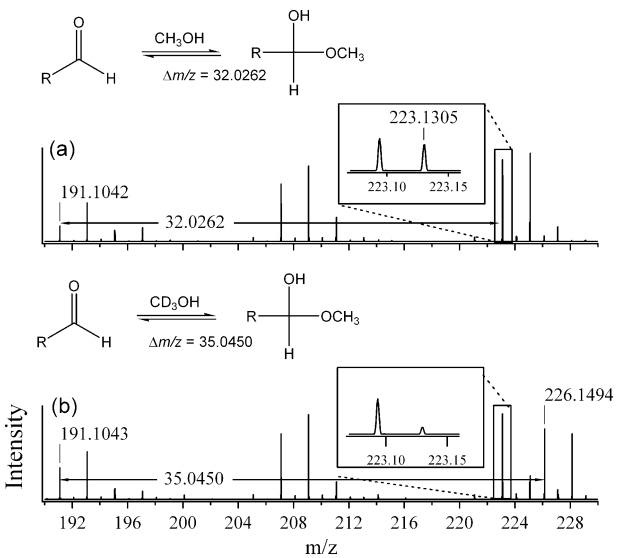

Fig. 10 Aldehyde constituents of SOA partially convert into hemiacetals as a result of their reaction with methanol solvent during ESI-MS analysis.[31]

Improving quantitative capabilities of HR-MS methods

Quantification of concentrations of analytes in complex mixtures based on the abundance of ions in mass spectra obtained using soft ionization techniques is challenging. Signal suppression resulting from matrix effects, significant variation in ionization efficiencies of different classes of compounds, and dependence of signal response on the presence of surfactant molecules are the major factors affecting absolute and relative abundances of ions.[82] However, a number of successful quantitative applications of ESI and DESI have been reported over the last few years. Oss *et al.* [144] developed a scale of ESI ionization efficiency using more than 60 standard compounds with different organic group functionalities under typical experimental conditions of ESI-MS analysis. The scale ranged over nearly six orders of magnitude, and was reasonably modeled by an empirical expression with only two critical parameters: pK_a and molecular volume of analyte molecules. Quantitative aspects of DESI-MS analysis have been also discussed in the literature,[145,146] including quantitative analysis of selected individual compounds in ambient OA samples.[99,100,147] Nevertheless, because of the complexity and wide variety of individual OA constituents, development of robust and reproducible methods for quantitative analysis of OA using ESI, DESI and related ionization approaches requires additional analysis and validation work.

Development of methods for HR-MS data interpretation

There is need for improved software tools for the HR-MS data analysis and interpretation, such as those being developed by the National High Magnetic Field Laboratory at Florida State University and by the Department of Energy's Biological MS Data and Software Distribution Center at the Pacific Northwest National Laboratory (PNNL). For example, VIPER (Visual Inspection of Peak/Elution Relationships) makes it possible to visualize large sets of LC-HR-MS data, Decon2LS and ICR2LS serve as powerful HR-MS peak detector tools, and Molecular Formula Calculator converts observed ionic masses into formulae while observing valence constraints. Notable examples of algorithm development for identification of molecular building blocks for natural organic matter samples include total mass difference statistics analysis[148] and C, H, O-compositional space analysis.[149]

There is also need to develop tools for prediction of high-resolution mass spectra from chemical principles. Although reliable predication of relative abundances of different compounds in OA would require prohibitively complicated chemical kinetics models, the occurrence of these compounds in OA may be predicted using a judiciously chosen set of chemical reactions and starting compounds. For example, we were able to match a significant fraction of observed monomers in the limonene SOA mass spectrum with a model that included known chemistry of carbonyl oxides, alkylperoxy, and alkoxy radicals.[30] We envision that in the future, standard atmospheric chemistry and organic chemistry mechanisms will be used to predict OA composition using chemoinformatics tools developed by combinatorial chemists (*e.g.*, ref. 150 and 151).

Complementary applications of HR-MS and other analytical techniques for aerosol analysis

Detailed understanding of the complex chemistry of organic aerosols and their environmental impacts is a challenging task because no single method of analytical chemistry is capable of providing the full range of needed information. While HR-MS approaches discussed in this review can provide detailed information on the molecular content of OA, these methods use bulk particle samples and provide no knowledge of the individual particle composition. In contrast, electron microscopy and micro-spectroscopy[152,153] visualize individual organic particles and their internal structures; however, they largely exclude molecular-level information, and are limited to elemental and chemical bonding characterization. Therefore, application of complementary analytical methods for OA analysis is necessary for comprehensive characterization of aerosol properties ranging from bulk molecular composition of complex OA mixtures to microscopy level details of individual particles. Combined assessment of the results provided by different analytical chemistry techniques will bring chemical analysis of OA to an unprecedented level of sophistication that will advance fundamental understanding of aerosol atmospheric chemistry.

Glossary of the acronyms used in the manuscript

APCI	atmospheric pressure chemical ionization
APPI	atmospheric pressure photo ionization
ASAP	atmospheric solid analysis probe
BBA	biomass burning aerosol(s)
CID	collision induced dissociation
DOM	dissolved organic matter
DAPCI	desorption atmospheric pressure chemical ionization
DART	direct analysis in real time
DESI	desorption electrospray ionization
ELDI	electrospray-assisted laser desorption and ionization
ESI	electrospray ionization
FT-ICR MS	Fourier-transform ion cyclotron resonance (mass spectrometry)
GC-MS	gas chromatography–mass spectrometry
High-MW	high molecular weight (compounds)
HR-MS	high resolution mass spectrometry
HULIS	humic like substances
KM	Kendrick mass
KMD	Kendrick mass defect
LC	liquid chromatography
LTQ/Orbitrap	(hybrid) linear trap quadrupole–Orbitrap (mass spectrometer)
MALDI	matrix assisted laser desorption ionization
MS/MS, MS^n	tandem mass spectrometry
nano-DESI	nanospray desorption electrospray ionization
NM	nominal mass
OA	organic aerosol(s)
PILS	particle into liquid sampler
POA	primary organic aerosol(s)
PPD	ponderosa pine duff

This journal is © the Owner Societies 2011

PPNS	ponderosa pine needles and sticks
QTOF	(hybrid) quadrupole-time of flight (mass spectrometer)
DBE	(ring and) double bond equivalent
SOA	secondary organic aerosol(s)
SPN	southern pine needles
TOF	time of flight
UV/Vis	ultraviolet–visible (spectrometer)
VK	van Krevelen (diagram)
VOC	volatile organic compound(s)
WSOC	water soluble organic carbon
WSON	water soluble organic nitrogen

Acknowledgements

The authors acknowledge financial support from the National Science Foundation (ATM-0831518 and CHE-0909227), the Chemical Sciences Division, Office of Basic Energy Sciences of the US DOE, and the intramural research and development program of the W. R. Wiley Environmental Molecular Sciences Laboratory (EMSL). EMSL is a national scientific user facility located at PNNL, and sponsored by the Office of Biological and Environmental Research of the US PNNL is operated for US DOE by Battelle Memorial Institute under Contract No. DE-AC06-76RL0 1830. The authors also thank their colleagues who profoundly influenced and co-authored individual projects conducted in the authors' groups and conveyed by this perspective manuscript: G. A. Anderson, A. P. Bateman, D. L. Bones, A. L. Chang-Graham, Y. Desyaterik, T. J. Johnson, L. Q. Nguyen, T. B. Nguyen, L. T. Profeta, P. J. Roach, G. W. Slysz, J. S. Smith, M. L. Walser, and R. J. Yokelson.

References

1 S. Solomon, D. Qin, M. Manning, Z. Chen, M. Marquis, K. B. Averyt, M. Tignor and H. L. Miller, *Climate Change 2007: The Physical Science Basis. Contribution of Working Group I to the Fourth Assessment Report of the Intergovernmental Panel on Climate Change*, Cambridge University Press, Cambridge, UK and New York, USA, 2007, p. 996.
2 J. L. Mauderly and J. C. Chow, *Inhalation Toxicol.*, 2008, **20**, 257–288.
3 F. W. Went, *Nature*, 1960, **187**, 641–643.
4 A. J. Haagen-Smit, *Ind. Eng. Chem.*, 1952, **44**, 1342–1346.
5 M. Hallquist, J. C. Wenger, U. Baltensperger, Y. Rudich, D. Simpson, M. Claeys, J. Dommen, N. M. Donahue, C. George, A. H. Goldstein, J. F. Hamilton, H. Herrmann, T. Hoffmann, Y. Iinuma, M. Jang, M. E. Jenkin, J. L. Jimenez, A. Kiendler-Scharr, W. Maenhaut, G. McFiggans, T. F. Mentel, A. Monod, A. S. H. Prevot, J. H. Seinfeld, J. D. Surratt, R. Szmigielski and J. Wildt, *Atmos. Chem. Phys.*, 2009, **9**, 5155–5236.
6 Y. Rudich, N. M. Donahue and T. F. Mentel, *Annu. Rev. Phys. Chem.*, 2007, **58**, 321–352.
7 J. L. Jimenez, M. R. Canagaratna, N. M. Donahue, A. S. H. Prevot, Q. Zhang, J. H. Kroll, P. F. DeCarlo, J. D. Allan, H. Coe, N. L. Ng, A. C. Aiken, K. S. Docherty, I. M. Ulbrich, A. P. Grieshop, A. L. Robinson, J. Duplissy, J. D. Smith, K. R. Wilson, V. A. Lanz, C. Hueglin, Y. L. Sun, J. Tian, A. Laaksonen, T. Raatikainen, J. Rautiainen, P. Vaattovaara, M. Ehn, M. Kulmala, J. M. Tomlinson, D. R. Collins, M. J. Cubison, E. J. Dunlea, J. A. Huffman, T. B. Onasch, M. R. Alfarra, P. I. Williams, K. Bower, Y. Kondo, J. Schneider, F. Drewnick, S. Borrmann, S. Weimer, K. Demerjian, D. Salcedo, L. Cottrell, R. Griffin, A. Takami, T. Miyoshi, S. Hatakeyama, A. Shimono, J. Y. Sun, Y. M. Zhang, K. Dzepina, J. R. Kimmel, D. Sueper, J. T. Jayne, S. C. Herndon, A. M. Trimborn, L. R. Williams, E. C. Wood, A. M. Middlebrook, C. E. Kolb, U. Baltensperger and D. R. Worsnop, *Science*, 2009, **326**, 1525–1529.
8 N. M. Donahue, A. L. Robinson and S. N. Pandis, *Atm. Environ.*, 2008, **43**, 94–106.
9 J. H. Kroll and J. H. Seinfeld, *Atmos. Environ.*, 2008, **42**, 3593–3624.
10 M. Claeys, B. Graham, G. Vas, W. Wang, R. Vermeylen, V. Pashynska, J. Cafmeyer, P. Guyon, M. O. Andreae, P. Artaxo and W. Maenhaut, *Science*, 2004, **303**, 1173–1176.
11 Y. Iinuma, O. Boge, A. Kahnt and H. Herrmann, *Phys. Chem. Chem. Phys.*, 2009, **11**, 7985–7997.
12 J. D. Surratt, J. H. Kroll, T. E. Kleindienst, E. O. Edney, M. Claeys, A. Sorooshian, N. L. Ng, J. H. Offenberg, M. Lewandowski, M. Jaoui, R. C. Flagan and J. H. Seinfeld, *Environ. Sci. Technol.*, 2007, **41**, 517–527.
13 D. S. Thomson, M. E. Schein and D. M. Murphy, *Aerosol Sci. Technol.*, 2000, **33**, 153–169.
14 Y. Su, M. F. Sipin, H. Furutani and K. A. Prather, *Anal. Chem.*, 2004, **76**, 712–719.
15 A. Zelenyuk and D. Imre, *Aerosol Sci. Technol.*, 2005, **39**, 554–568.
16 B. Oektem, M. P. Tolocka and M. V. Johnston, *Anal. Chem.*, 2004, **76**, 253–261.
17 P. F. DeCarlo, J. R. Kimmel, A. Trimborn, M. J. Northway, J. T. Jayne, A. C. Aiken, M. Gonin, K. Fuhrer, T. Horvath, K. S. Docherty, D. R. Worsnop and J. L. Jimenez, *Anal. Chem.*, 2006, **78**, 8281–8289.
18 D. C. Sykes, E. Woods, III, G. D. Smith, T. Baer and R. E. Miller, *Anal. Chem.*, 2002, **74**, 2048–2052.
19 J. N. Smith, K. F. Moore, P. H. McMurry and F. L. Eisele, *Aerosol Sci. Technol.*, 2004, **38**, 100–110.
20 J. D. Hearn and G. D. Smith, *Anal. Chem.*, 2004, **76**, 2820–2826.
21 A. G. Marshall and R. P. Rodgers, *Acc. Chem. Res.*, 2004, **37**, 53–59.
22 E. B. Kujawinski, P. G. Hatcher and M. A. Freitas, *Anal. Chem.*, 2002, **74**, 413–419.
23 A. G. Marshall and R. P. Rodgers, *Proc. Natl. Acad. Sci. U. S. A.*, 2008, **105**, 18090–18095.
24 E. Bae, J. G. Na, S. H. Chung, H. S. Kim and S. Kim, *Energy Fuels*, 2010, **24**, 2563–2569.
25 S. Kim, R. P. Rodgers and A. G. Marshall, *Int. J. Mass Spectrom.*, 2006, **251**, 260–265.
26 A. L. Chang-Graham, L. T. Profeta, T. J. Johnson, R. J. Yokelson, A. Laskin and J. Laskin, *Environ. Sci. Technol.*, 2011, DOI: 10.1021/es1003010J, in press.
27 M. P. Tolocka, M. Jang, J. M. Ginter, F. J. Cox, R. M. Kamens and M. V. Johnston, *Environ. Sci. Technol.*, 2004, **38**, 1428–1434.
28 T. Reemtsma, A. These, P. Venkatachari, X. Y. Xia, P. K. Hopke, A. Springer and M. Linscheid, *Anal. Chem.*, 2006, **78**, 8299–8304.
29 A. Reinhardt, C. Emmenegger, B. Gerrits, C. Panse, J. Dommen, U. Baltensperger, R. Zenobi and M. Kalberer, *Anal. Chem.*, 2007, **79**, 4074–4082.
30 M. L. Walser, Y. Desyaterik, J. Laskin, A. Laskin and S. A. Nizkorodov, *Phys. Chem. Chem. Phys.*, 2008, **10**, 1009–1022.
31 A. P. Bateman, M. L. Walser, Y. Desyaterik, J. Laskin, A. Laskin and S. A. Nizkorodov, *Environ. Sci.Technol.*, 2008, **42**, 7341–7346.
32 A. Sadezky, R. Winterhalter, B. Kanawati, A. Rompp, B. Spengler, A. Mellouki, G. Le Bras, P. Chaimbault and G. K. Moortgat, *Atmos. Chem. Phys.*, 2008, **8**, 2667–2699.
33 A. S. Wozniak, J. E. Bauer, R. L. Sleighter, R. M. Dickhut and P. G. Hatcher, *Atmos. Chem. Phys.*, 2008, **8**, 5099–5111.
34 Y. Gomez-Gonzalez, J. D. Surratt, F. Cuyckens, R. Szmigielski, R. Vermeylen, M. Jaoui, M. Lewandowski, J. H. Offenberg, T. E. Kleindienst, E. O. Edney, F. Blockhuys, C. Van Alsenoy, W. Maenhaut and M. Claeys, *J. Mass Spectrom.*, 2008, **43**, 371–382.
35 K. E. Altieri, S. P. Seitzinger, A. G. Carlton, B. J. Turpin, G. C. Klein and A. G. Marshall, *Atmos. Environ.*, 2008, **42**, 1476–1490.
36 M. J. Perri, S. Seitzinger and B. J. Turpin, *Atmos. Environ.*, 2009, **43**, 1487–1497.
37 L. Muller, M. C. Reinnig, H. Hayen and T. Hoffmann, *Rapid Commun. Mass Spectrom.*, 2009, **23**, 971–979.

38 K. E. Altieri, B. J. Turpin and S. P. Seitzinger, *Atmos. Chem. Phys.*, 2009, **9**, 2533–2542.
39 A. P. Bateman, S. A. Nizkorodov, J. Laskin and A. Laskin, *Phys. Chem. Chem. Phys.*, 2009, **11**, 7931–7942.
40 K. J. Heaton, R. L. Sleighter, P. G. Hatcher, W. A. Hall and M. V. Johnston, *Environ. Sci. Technol.*, 2009, **43**, 7797–7802.
41 J. S. Smith, A. Laskin and J. Laskin, *Anal. Chem.*, 2009, **81**, 1512–1521.
42 A. Laskin, J. S. Smith and J. Laskin, *Environ. Sci. Technol.*, 2009, **43**, 3764–3771.
43 K. E. Altieri, B. J. Turpin and S. P. Seitzinger, *Environ. Sci. Technol.*, 2009, **43**, 6950–6955.
44 T. B. Nguyen, A. P. Bateman, D. L. Bones, S. A. Nizkorodov, J. Laskin and A. Laskin, *Atmos. Environ.*, 2010, **44**, 1032–1042.
45 J. Laskin, A. Laskin, P. J. Roach, G. W. Slysz, G. A. Anderson, S. A. Nizkorodov, D. L. Bones and L. Q. Nguyen, *Anal. Chem.*, 2010, **82**, 2048–2058.
46 L. R. Mazzoleni, B. M. Ehrmann, X. H. Shen, A. G. Marshall and J. L. Collett, *Environ. Sci. Technol.*, 2010, **44**, 3690–3697.
47 M. J. Perri, Y. B. Lim, S. P. Seitzinger and B. J. Turpin, *Atmos. Environ.*, 2010, **44**, 2658–2664.
48 P. J. Roach, J. Laskin and A. Laskin, *Anal. Chem.*, 2010, **82**, 7979–7986.
49 W. A. Hall and M. V. Johnston, *Aerosol Sci. Technol.*, 2010, in press.
50 A. P. Bateman, S. A. Nizkorodov, J. Laskin and A. Laskin, *Anal. Chem.*, 2010, **82**, 8010–8016.
51 Y. Gao, W. A. Hall and M. V. Johnston, *Environ. Sci. Technol.*, 2010, DOI: 10.1021/es101861k, Article ASAP.
52 D. L. Bones, J. Laskin, A. Laskin and S. A. Nizkorodov, 2011, in preparation.
53 P. Schmitt-Kopplin, A. Gelencser, E. Dabek-Zlotorzynska, G. Kiss, N. Hertkorn, M. Harir, Y. Hong and I. Gebefűgi, *Anal. Chem.*, 2010, **82**, 8017–8026.
54 S. A. McLuckey and J. M. Wells, *Chem. Rev.*, 2001, **101**, 571–606.
55 A. G. Marshall and C. L. Hendrickson, *Annu. Rev. Anal. Chem.*, 2008, **1**, 579–599.
56 I. V. Chernushevich, A. V. Loboda and B. A. Thomson, *J. Mass Spectrom.*, 2001, **36**, 849–865.
57 R. H. Perry, R. G. Cooks and R. J. Noll, *Mass Spectrom. Rev.*, 2008, **27**, 661–699.
58 A. Makarov, E. Denisov, A. Kholomeev, W. Baischun, O. Lange, K. Strupat and S. Horning, *Anal. Chem.*, 2006, **78**, 2113–2120.
59 A. Makarov, E. Denisov and O. Lange, *J. Am. Soc. Mass Spectrom.*, 2009, **20**, 1391–1396.
60 L. K. Zhang, D. Rempel, B. N. Pramanik and M. L. Gross, *Mass Spectrom. Rev.*, 2005, **24**, 286–309.
61 A. G. Marshall, *Int. J. Mass Spectrom.*, 2000, **200**, 331–356.
62 T. M. Schaub, C. L. Hendrickson, S. Horning, J. P. Quinn, M. W. Senko and A. G. Marshall, *Anal. Chem.*, 2008, **80**, 3985–3990.
63 F. He, C. L. Hendrickson and A. G. Marshall, *Anal. Chem.*, 2000, **73**, 647–650.
64 A. Makarov, *Anal. Chem.*, 2000, **72**, 1156–1162.
65 A. G. Marshall, C. L. Hendrickson and G. S. Jackson, *Mass Spectrom. Rev.*, 1998, **17**, 1–35.
66 M. L. Vestal, *J. Mass Spectrom.*, 2009, **44**, 303–317.
67 C. A. Hughey, R. P. Rodgers and A. G. Marshall, *Anal. Chem.*, 2002, **74**, 4145–4149.
68 S. Kim, R. W. Kramer and P. G. Hatcher, *Anal. Chem.*, 2003, **75**, 5336–5344.
69 J. Laskin and J. H. Futrell, *Mass Spectrom. Rev.*, 2005, **24**, 135–167.
70 S. A. McLuckey and D. E. Goeringer, *J. Mass Spectrom.*, 1997, **32**, 461–474.
71 J. Laskin and J. H. Futrell, *Mass Spectrom. Rev.*, 2003, **22**, 158–181.
72 J. V. Olsen, B. Macek, O. Lange, A. Makarov, S. Horning and M. Mann, *Nat. Methods*, 2007, **4**, 709–712.
73 T. Guo, C. S. Gan, H. Zhang, Y. Zhu, O. L. Kon and S. K. Sze, *J. Proteome Res.*, 2008, **7**, 4831–4840.
74 V. Grill, J. Shen, C. Evans and R. G. Cooks, *Rev. Sci. Instrum.*, 2001, **72**, 3149–3179.
75 V. H. Wysocki, K. E. Joyce, C. M. Jones and R. L. Beardsley, *J. Am. Soc. Mass Spectrom.*, 2008, **19**, 190–208.
76 R. C. Dunbar, *Int. J. Mass Spectrom.*, 2000, **200**, 571–589.
77 J. B. Fenn, M. Mann, C. K. Meng, S. F. Wong and C.M. Whitehouse, *Mass Spectrom. Rev.*, 1990, **9**, 37–70.
78 W. C. Byrdwell, *Lipids*, 2001, **36**, 327–346.
79 D. B. Robb, T. R. Covey and A. P. Bruins, *Anal. Chem.*, 2000, **72**, 3653–3659.
80 F. Hillenkamp, M. Karas, R. C. Beavis and B. T. Chait, *Anal. Chem.*, 1991, **63**, A1193–A1202.
81 R. G. Cooks, Z. Ouyang, Z. Takats and J. M. Wiseman, *Science*, 2006, **311**, 1566–1570.
82 P. Kebarle and U. H. Verkerk, in *Electrospray and MALDI Mass Spectrometry Fundamentals, Instrumentation, Practicalities, and Biological Applications*, ed. R. B. Cole, John Wiley & Sons, Inc., Hoboken, NJ, 2nd edn, 2010.
83 S. S. Cai and J. A. Syage, *Anal. Chem.*, 2006, **78**, 1191–1199.
84 M. Kalberer, M. Sax and V. Samburova, *Environ. Sci. Technol.*, 2006, **40**, 5917–5922.
85 G. J. Van Berkel, S. P. Pasilis and O. Ovchinnikova, *J. Mass Spectrom.*, 2008, **43**, 1161–1180.
86 H. Chen, G. Gamez and R. Zenobi, *J. Am. Soc. Mass Spectrom.*, 2009, **20**, 1947–1963.
87 D. R. Ifa, C. P. Wu, Z. Ouyang and R. G. Cooks, *Analyst*, 2010, **135**, 669–681.
88 D. J. Weston, *Analyst*, 2010, **135**, 661–668.
89 Z. Takats, J. M. Wiseman, B. Gologan and R. G. Cooks, *Science*, 2004, **306**, 471–473.
90 Z. Takats, J. M. Wiseman and R. G. Cooks, *J. Mass Spectrom.*, 2005, **40**, 1261–1275.
91 R. B. Cody, J. A. Laramee and H. D. Durst, *Anal. Chem.*, 2005, **77**, 2297–2302.
92 Z. Takats, I. Cotte-Rodriguez, N. Talaty, H. W. Chen and R. G. Cooks, *Chem. Commun.*, 2005, 1950–1952.
93 J. Shiea, M. Z. Huang, H. J. Hsu, C. Y. Lee, C. H. Yuan, I. Beech and J. Sunner, *Rapid Commun. Mass Spectrom.*, 2005, **19**, 3701–3704.
94 J. D. Harper, N. A. Charipar, C. C. Mulligan, X. Zhang, R. G. Cooks and Z. Ouyang, *Anal. Chem.*, 2008, **80**, 9097–9104.
95 C. N. McEwen, R. G. McKay and B. S. Larsen, *Anal. Chem.*, 2005, **77**, 7826–7831.
96 J. S. Sampson, A. M. Hawkridge and D. C. Muddiman, *J. Am. Soc. Mass Spectrom.*, 2006, **17**, 1712–1716.
97 L. Nyadong, A. S. Galhena and F. M. Fernandez, *Anal. Chem.*, 2009, **81**, 7788–7794.
98 S. C. Cheng, T. L. Cheng, H. C. Chang and J. Shiea, *Anal. Chem.*, 2009, **81**, 868–874.
99 M. Li, H. Chen, X. Yang, J. M. Chen and C. L. Li, *Atmos. Environ.*, 2009, **43**, 2717–2720.
100 M. Li, H. Chen, B. F. Wang, X. Yang, J. J. Lian and J. M. Chen, *Int. J. Mass Spectrom.*, 2009, **281**, 31–36.
101 E. A. Bruns, V. Perraud, J. Greaves and B. J. Finlayson-Pitts, *Anal. Chem.*, 2010, **82**, 5922–5927.
102 P. J. Roach, J. Laskin and A. Laskin, *Analyst*, 2010, **135**, 2233–2236.
103 C. A. Hughey, C. L. Hendrickson, R. P. Rodgers, A. G. Marshall and K. N. Qian, *Anal. Chem.*, 2001, **73**, 4676–4681.
104 E. Kendrick, *Anal. Chem.*, 1963, **35**, 2146–2154.
105 J. Meija, *Anal. Bioanal. Chem.*, 2006, **385**, 486–499.
106 C. S. Hsu, K. N. Qian and Y. N. C. Chen, *Anal. Chim. Acta*, 1992, **264**, 79–89.
107 A. C. Stenson, A. G. Marshall and W. T. Cooper, *Anal. Chem.*, 2003, **75**, 1275–1284.
108 T. Kind and O. Fiehn, *BMC Bioinformatics*, 2007, **8**, 1–20.
109 F. W. McLafferty and F. Turecek, *Interpretation of Mass Spectra*, University Science Books, Mill Valley, CA, 1993.
110 T. Reemtsma, *J. Mass Spectrom*, 2010, **45**, 382–390.
111 A. C. Aiken, P. F. DeCarlo and J. L. Jimenez, *Anal. Chem.*, 2007, **79**, 8350–8358.
112 A. C. Aiken, P. F. Decarlo, J. H. Kroll, D. R. Worsnop, J. A. Huffman, K. S. Docherty, I. M. Ulbrich, C. Mohr, J. R. Kimmel, D. Sueper, Y. Sun, Q. Zhang, A. Trimborn, M. Northway, P. J. Ziemann, M. R. Canagaratna, T. B. Onasch, M. R. Alfarra, A. S. H. Prevot, J. Dommen, J. Duplissy, A. Metzger, U. Baltensperger and J. L. Jimenez, *Environ. Sci. Technol.*, 2008, **42**, 4478–4485.
113 Z. Wu, R. P. Rodgers and A. G. Marshall, *Anal. Chem.*, 2004, **76**, 2511–2516.

 This journal is © the Owner Societies 2011

114 X. Pan, J. S. Underwood, J.-H. Xing, S. A. Mang and S. A. Nizkorodov, *Atmos. Chem. Phys.*, 2009, **9**, 3851–3865.
115 A. Jordan, S. Haidacher, G. Hanel, E. Hartungen, J. Herbig, L. Maerk, R. Schottkowsky, H. Seehauser, P. Sulzer and T. D. Maerk, *Int. J. Mass Spectrom.*, 2009, **286**, 32–38.
116 R. J. Weber, D. Orsini, Y. Daun, Y. N. Lee, P. J. Klotz and F. Brechtel, *Aerosol Sci. Technol.*, 2001, **35**, 718–727.
117 T. Wainman, J. Zhang, C. J. Weschler and P. J. Lioy, *Environ. Health Persp.*, 2000, **108**, 1139–1145.
118 A. Guenther, T. Karl, P. Harley, C. Wiedinmyer, P. I. Palmer and C. Geron, *Atmos. Chem. Phys.*, 2006, **6**, 3181–3210.
119 K. C. Barsanti and J. F. Pankow, *Atmos. Environ.*, 2004, **38**, 4371–4382.
120 K. C. Barsanti and J. F. Pankow, *Atmos. Environ.*, 2005, **39**, 6597–6607.
121 J. H. Kroll, N. L. Ng, S. M. Murphy, V. Varutbangkul, R. C. Flagan and J. H. Seinfeld, *J. Geophys. Res.*, 2005, **110**, D23207, DOI: 23210.21029/22005JD006004.
122 D. L. Bones, D. K. Henricksen, S. A. Mang, M. Gonsior, A. P. Bateman, T. B. Nguyen, W. J. Cooper and S. A. Nizkorodov, *J. Geophys. Res.*, 2010, **115**, D05203, DOI: 05210.01029/02009JD012864.
123 M. O. Andreae and A. Gelencser, *Atmos. Chem. Phys.*, 2006, **6**, 3131–3148.
124 X. F. Wang, S. Gao, X. Yang, H. Chen, J. M. Chen, G. S. Zhuang, J. D. Surratt, M. N. Chan and J. H. Seinfeld, *Environ. Sci. Technol.*, 2010, **44**, 4441–4446.
125 Y. Pang, B. Turpin and L. Gundel, *Aerosol Sci. Technol.*, 2006, **40**, 128–133.
126 B. J. Turpin and H.-J. Lim, *Aerosol Sci. Technol.*, 2001, **35**, 602–610.
127 B. R. T. Simoneit, *Appl. Geochem.*, 2002, **17**, 129–162.
128 H. H. Perkampus, *UV-Vis Atlas of Organic Compounds*, Weinheim, New York, 1992.
129 T. Raatikainen, P. Vaattovaara, P. Tiitta, P. Miettinen, J. Rautiainen, M. Ehn, M. Kulmala, A. Laaksonen and D. R. Worsnop, *Atmos. Chem. Phys.*, 2010, **10**, 2063–2077.
130 A. C. Aiken, B. de Foy, C. Wiedinmyer, P. F. DeCarlo, I. M. Ulbrich, M. N. Wehrli, S. Szidat, A. S. H. Prevot, J. Noda, L. Wacker, R. Volkamer, E. Fortner, J. Wang, A. Laskin, V. Shutthanandan, J. Zheng, R. Zhang, G. Paredes-Miranda, W. P. Arnott, L. T. Molina, G. Sosa, X. Querol and J. L. Jimenez, *Atmos. Chem. Phys.*, 2010, **10**, 5315–5341.
131 A. C. Aiken, D. Salcedo, M. J. Cubison, J. A. Huffman, P. F. DeCarlo, I. M. Ulbrich, K. S. Docherty, D. Sueper, J. R. Kimmel, D. R. Worsnop, A. Trimborn, M. Northway, E. A. Stone, J. J. Schauer, R. M. Volkamer, E. Fortner, B. de Foy, J. Wang, A. Laskin, V. Shutthanandan, J. Zheng, R. Zhang, J. Gaffney, N. A. Marley, G. Paredes-Miranda, W. P. Arnott, L. T. Molina, G. Sosa and J. L. Jimenez, *Atmos. Chem. Phys.*, 2009, **9**, 6633–6653.
132 K. Levsel, H. M. Schiebel, J. K. Terlouw, K. J. Jobst, M. Elend, A. Preib, H. Thiele and A. Ingendoh, *J. Mass Spectrom.*, 2007, **42**, 1024–1044.
133 E. R. Graber and Y. Rudich, *Atmos. Chem. Phys.*, 2006, **6**, 729–753.
134 S. Cornell, K. Mace, S. Coeppicus, R. Duce, B. Huebert, T. Jickells and L. Z. Zhuang, *J. Geophys. Res.*, 2001, **106**, 7973–7983.
135 S. E. Cornell, T. D. Jickells, J. N. Cape, A. P. Rowland and R. A. Duce, *Atmos. Environ.*, 2003, **37**, 2173–2191.
136 K. A. Mace, P. Artaxo and R. A. Duce, *J. Geophys. Res.*, 2003, **108**, 4512, DOI: 4510.1029/2003JD003557.
137 K. A. Mace, R. A. Duce and N. W. Tindale, *J. Geophys. Res.*, 2003, **108**, 4338, DOI: 4310.1029/2002JD003051.
138 F. S. I. Chapin, P. A. Matson and H. A. Mooney, *Principles of Terrestrial Ecosystem Ecology*, Springer Verlag, New York, 2002.
139 K. A. Prather, C. D. Hatch and V. H. Grassian, *Annu. Rev. Anal. Chem.*, 2008, **1**, 485–514.
140 A. Laskin, M. J. Iedema and J. P. Cowin, *Aerosol Sci. Technol.*, 2003, **37**, 246–260.
141 H. W. Gu, B. Hu, J. Q. Li, S. P. Yang, J. Han and H. W. Chen, *Analyst*, 2010, **135**, 1259–1267.
142 L. Nyadong, E. Hohenstein, A. Galhena, A. Lane, J. Kubanek, C. Sherrill and F. Fernández, *Anal. Bioanal. Chem.*, 2009, **394**, 245–254.
143 J. D. Surratt, S. M. Murphy, J. H. Kroll, N. L. Ng, L. Hildebrandt, A. Sorooshian, R. Szmigielski, R. Vermeylen, W. Maenhaut, M. Claeys, R. C. Flagan and J. H. Seinfeld, *J. Phys. Chem. A*, 2006, **110**, 9665–9690.
144 M. Oss, A. Kruve, K. Herodes and I. Leito, *Anal. Chem.*, 2010, **82**, 2865–2872.
145 D. R. Ifa, N. E. Manicke, A. L. Rusine and R. G. Cooks, *Rapid Commun. Mass Spectrom.*, 2008, **22**, 503–510.
146 L. Nyadong, S. Late, M. D. Green, A. Banga and F. M. Fernandez, *J. Am. Soc. Mass Spectrom.*, 2008, **19**, 380–388.
147 H. Chen, M. Li, Y. P. Zhang, X. Yang, J. J. Lian and J. M. Chen, *J. Am. Soc. Mass Spectrom.*, 2008, **19**, 450–454.
148 E. V. Kunenkov, A. S. Kononikhin, I. V. Perminova, N. Hertkorn, A. Gaspar, P. Schmitt-Kopplin, I. A. Popov, A. V. Garmash and E. N. Nikolaev, *Anal. Chem.*, 2009, **81**, 10106–10115.
149 N. Hertkorn, M. Frommberger, M. Witt, B. P. Koch, P. Schmitt-Kopplin and E. M. Perdue, *Anal. Chem.*, 2008, **80**, 8908–8919.
150 J. H. Chen and P. Baldi, *J. Chem. Educ.*, 2008, **85**, 1699–1703.
151 J. H. Chen and P. Baldi, *J. Chem. Inf. Model.*, 2009, **49**, 2034–2043.
152 R. C. Moffet, T. Henn, A. Laskin and M. K. Gilles, *Anal. Chem.*, 2010, **82**, 7906–7914.
153 R. C. Moffet, T. R. Henn, A. V. Tivanski, R. J. Hopkins, Y. Desyaterik, A. L. D. Kilcoyne, T. Tyliszczak, J. Fast, J. Barnard, V. Shutthanandan, S. S. Cliff, K. D. Perry, A. Laskin and M. K. Gilles, *Atmos. Chem. Phys.*, 2010, **10**, 961–976.